Research on Fuzzy-PID Control System for Mecanum Robot

Submitted: 11th July 2024; accepted: 3rd September 2024

Trong-Tai Nguyen, Quang-Tho Le, Quang-Phuoc Pham, Tran-Long Le

DOI: 10.14313/jamris-2026-039

Abstract:
In this paper, a comprehensive control system for precise motion control and trajectory tracking of Four Mecanum-Wheeled Mobile Robots (FMWMRs) is presented. The proposed approach addresses issues including non-linearities, uncertainties, and external disturbances by combining a fuzzy logic controller for orientation control and a fuzzy-PID controller for position control. The dynamic model of the FMWMR is summarized. For localization and heading angle estimates, an IMU sensor and a camera are leveraged, and a complementary filter method is utilized for the best possible sensor fusion. A real-world FMWMR prototype and extensive Matlab/Simulink simulations show how reliable and effective the control system is at providing accurate trajectory tracking with low RMS errors under a range of loading scenarios. With possible applications in material handling, mobile robotics, and industrial automation, the suggested approach provides a dependable solution for trajectory tracking and motion control in FMWMRs.

Keywords: *Mecanum wheel, Fuzzy logic control, Fuzzy-PID control, trajectory tracking, sensor fusion*

1. Introduction

Nowadays, the demand for mobile robots is rising as they have the potential to free humans from repetitive, dangerous, and labor-intensive tasks [1–4]. In industries such as manufacturing, logistics, and healthcare [5, 6], mobile robots are increasingly utilized for tasks like assembly line work, warehouse management, and patient transport. By taking over these duties, mobile robots not only enhance efficiency and productivity but also reduce the risk of injuries and allow human workers to focus on more complex and creative activities. Thanks to their remarkable omnidirectional mobility, four Mecanum-Wheeled Mobile Robots (FMWMRs) have garnered significant interest across various sectors, including military and industrial applications [7–9]. With special design of mecanum wheel, it allows the robots to navigate confined and intricate spaces with ease, making them highly useful in various fields such as industrial automation, warehouse operations, and search and rescue efforts [10]. Through the independent control of speed and direction for each wheel, this configuration enables FMWMRs to maneuver instantly in any direction from any starting orientation, eliminating the requirement for pre-orientation. As a result, compared to conventional platforms, these vehicles have excellent mobility and are well-suited for operations in confined places or crowded areas [7].

However, achieving accurate trajectory tracking and motion control of such platforms remains a challenge due to parameter uncertainties, non-linearities, external disturbances and the need for robust control strategies. These factors can further degrade the control performance. As a result, there are many problems that need to be solved when implementing a Mecanum robot project, such as control algorithm problems, position and rotation angle determination problems and so on [9, 11–14]. Many research works have been conducted to develop and implement different kinds of control techniques , such as: PID control [15, 16], backstepping control [17], sliding mode control [18], intelligent control based on neural networks [19, 20].

Fuzzy PID controllers are applied in various fields, including robotics, industrial automation, and process control, where system conditions are constantly changing and require adaptive control strategies. A Fuzzy PID controller combines the principles of a conventional PID (Proportional-Integral-Derivative) controller with fuzzy logic to improve performance in systems with non-linearity, uncertainties, or varying dynamics. Compared to conventional PID controllers, the Fuzzy PID controller demonstrates superior characteristics such as better handling of non-linearities, robustness in conditions of system uncertainty, and effective adaptation to dynamic environments without needing a precise mathematical model. Thanks to these advantages, Fuzzy PID controllers have been extensively investigated in numerous research studies [16, 21–26]. In [16, 21–23, 27], the Fuzzy PID controller was employed to control the mobile robot in condition of uncertainty factors such as friction, disturbance, and the robot's nonlinearity. While in [24–26], the fuzzy PID is applied in some other fields such as a permanent magnet synchronous motor, transformer coil temperature or active suspension.

For effective trajectory tracking and motion control in FMWMRs or mobile robots, precise localization and heading angle estimation need to be determined. Robot positioning and heading angle fusion methods play a crucial role in enhancing the accuracy and reliability of robotic navigation systems. Common positioning approaches include GPS [2], inertial sensors - IMU [28, 29], and vision systems [28, 30], LiDAR [31–33]. Especially, for indoor robot positioning, various methods have been explored, including IMU (Inertial Measurement Unit) and its sensor fusion techniques, ultrasonic sensors, infrared sensors, vision-based systems, radio frequency technologies, and LiDAR. The technologies, along with the advantages and drawbacks of each method, of these methods are discussed in [31, 34, 35]. Additionally, various fusion algorithms, such as Kalman filters [36], hidden Markov model [37, 38] or Bayesian estimation [2, 28, 39–41], are utilized to merge sensor data and reduce errors. Besides, to measure the robot's orientation, the IMU, which combines a magnetometer, accelerometer, and gyroscope, is extensively used. Well-known methods for calculating the heading angle with an IMU include the Complementary filter [29], Extended Kalman filter [28, 41, 42], Madgwick filter [43, 44] and Mahony filter [45]. However, IMUs have intrinsic limitations, including drift overtime due to cumulative sensor errors and vulnerability to external environmental factors like magnetic interference. To address these drawbacks, sensor fusion methods are employed to combine IMU data with other sensor inputs, enhancing overall reliability and performance.

In this paper, a comprehensive control system is investigated to achieve precise tracking control of FMWMRs. The controller structure is composed of a Fuzzy logic controller for orientation control and a Fuzzy-PID controller for position control. Through this integration, the trajectory tracking and motion control performance of FMWMRs are significantly improved. Velocities along the x and y axes are computed by the Fuzzy-PID controller based on position error and its derivative, while angular velocity is determined by the Fuzzy logic controller using the error and derivative of the heading angle. These computed velocities are subsequently utilized as inputs to inverse kinematic equations to derive the necessary wheel velocities. System nonlinearities and uncertainties are effectively managed and compensated by the fuzzy rule base through expert tuning.

To evaluate the control performance, extensive simulations were conducted in the Matlab/Simulink environment. The PID and Fuzzy controllers were also implemented to assess the superiority of the Fuzzy-PID approach. Additionally, a real-life FMWMR prototype was constructed to verify the effectiveness of the proposed controller under practical conditions. For obtaining the FMWMR's position and heading angle, a vision technique based on ArUco markers [46, 47] is employed. However, challenges such as sensitivity to lighting conditions and slow response rates are encountered with this approach. To address these limitations, an IMU is integrated with the ArUco marker detection results using a complementary filter [29], thereby improving the response and accuracy of the heading angle estimation. The overall of control approach and sensor fusion methodology can be illustrated in a comprehensive way as shown in Figure 1. The simulation and experimental results demonstrate the superiority of the proposed control system in achieving precise trajectory tracking and motion control for FMWMRs in both simulation and real-world scenarios.

The subsequent parts of this paper are organized as follows: Section II summarizes the mathematical model of a FMWMR. Section III details all the steps in Fuzzy and Fuzzy-PID design process. The method of positioning and orientation determination by sensor fusion is then illustrated in Section IV. Simulation, experiment results and discussion are shown in Section V. Finally, Section VI concludes our research and provides future directions for development.

2. Mathematical model

In this research, the mathematical model of FMWMR in [48] is used. In which, the kinematic model and dynamic model of FMWMR can be summarized as:

The robot kinematic model:

$$\dot{\theta}_w = \frac{J}{r_w}\dot{\varphi}_r \tag{1}$$

The robot's inverse kinematic model:

$$\dot{\varphi}_r = r_w J^+ \dot{\theta}_w \tag{2}$$

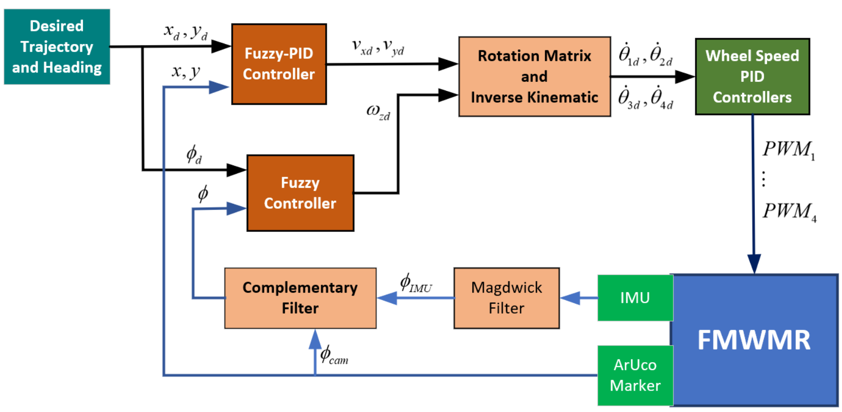

Figure 1. Overall structure of the proposed control system

In world frame – as shown in Figure 2, the robot motion is determined as:

$$\dot{\varphi}_q = \Re(\phi)\dot{\varphi}_r \tag{3}$$

where:

$\varphi_q=[x_q\ y_q\ \phi]^T$ is a vector of robot motion in inertia frame; $\varphi_r=[x_r\ y_r\ \phi]^T$ is a vector robot motion in robot frame; $\theta_w=[\theta_{w1}\ \theta_{w2}\ \theta_{w3}\ \theta_{w4}]^T$ is a vector of rotation angle of robot wheels; ϕ is robot heading angle; r_w is radius of mecanum wheel.

J is geometry matrix of robot; J^+ is inverse matrix of J

$$J = \begin{bmatrix} 1 & 1 & (a+b) \\ -1 & 1 & -(a+b) \\ 1 & 1 & -(a+b) \\ -1 & 1 & (a+b) \end{bmatrix}; J^+ = \begin{bmatrix} 1 & -1 & 1 & -1 \\ 1 & 1 & 1 & 1 \\ \frac{1}{a+b} & \frac{-1}{a+b} & \frac{-1}{a+b} & \frac{1}{a+b} \end{bmatrix}$$

a and b are haft of width and length of the robot flatform; $\Re(\phi)$ is frame convert matrix, which is determined as:

$$\Re(\phi) = \begin{bmatrix} \cos(\phi) & -\sin(\phi) & 0 \\ \sin(\phi) & \cos(\phi) & 0 \\ 0 & 0 & 1 \end{bmatrix} \tag{4}$$

The dynamic model of FMWMR is determined as:

$$\tau = M\ddot{\theta}_w + D_{\theta_w}\dot{\theta}_w + F \tag{5}$$

where: $\tau=[\tau_1\ \tau_2\ \tau_3\ \tau_4]^T$ is a vector of applied torque generated by robot wheel motors; $F=[F_1\ F_2\ F_3\ F_4]$; with $F_i = f_i \operatorname{sgn}(\dot{\theta}_{wi}); i \div 1:4$ represents the static friction on mecanum wheels.

3. Controller Design

For FMWMRs to operate well, trajectory tracking and motion control need a resilient and flexible control system that can deal with uncertainties, nonlinearities, and external disturbances. A hierarchical of control architecture that includes a fuzzy-PID controller for position control with a fuzzy logic controller for orientation control is investigated in order to overcome these issues. While the Fuzzy-PID controller is responsible for regulating the robot's position, the Fuzzy logic controller is designed to control the robot's heading angle, guaranteeing precise orientation tracking. The overall block diagram of the control system is illustrated in Figure 3. Each controller's design process will be detailed in the following subsections, beginning with the fuzzy controller used for orientation control.

3.1. Fuzzy logic controller for orientation control

To control the robot's orientation, a fuzzy logic controller is designed with two inputs and one output, as shown in Figure 4. The inputs consist of the heading angle error between the desired orientation and the robot's orientation ($e_\phi = \phi_d - \phi$) and its derivative (de_ϕ). The output is the desired angular velocity of the robot. Since the inputs and output of the fuzzy logic controller operate within different physical ranges, significant time is required to adjust the fuzzy logic for each variable in varying situations. To address this, in this research, all inputs and outputs of the fuzzy controller are normalized to the standard range [-1, 1] using normalization gains. This normalization simplifies the formulation of the fuzzy rule base and provides flexibility in adjusting input and output ranges during performance evaluation and tuning. By adjusting the normalization gains, the expected range can be modified, enabling the designed membership functions to automatically adapt to the new range without requiring a complete redesign.

Fuzzification

The design approach for the heading angle fuzzy controller begins with fuzzification. In this step, the crisp input values are converted into fuzzy sets using membership functions. Trapezoidal and triangular membership functions are used in this design due to their simplicity and ability to clearly represent the input and output spaces.

Based on experience from simulation and experiment results, the fuzzy inputs are fuzzified using seven membership functions: BN (Big Negative), MN (Medium Negative), SN (Small Negative), ZE (Zero), SP (Small Positive), MP (Medium Positive), and BP (Big Positive). The distribution of the membership functions of each input is illustrated in Figure 5 and Figure 6.

Similarly, for the fuzzy output, the angular velocity is fuzzified using seven membership functions: BN (Big Negative), MN (Medium Negative), SN (Small Negative), ZE (Zero), SP (Small Positive), MP (Medium Positive), BP (Big Positive). The distribution of these membership functions is illustrated in Figure 7.

The normalization gains for inputs and outputs of orientation controller are selected and presented as Table 1.

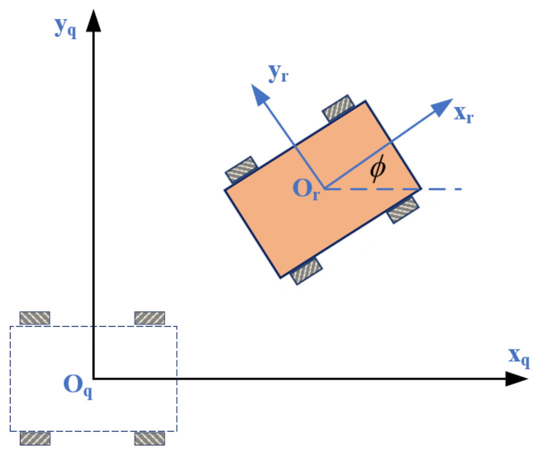

Figure 2. Robot in world frame and robot frame

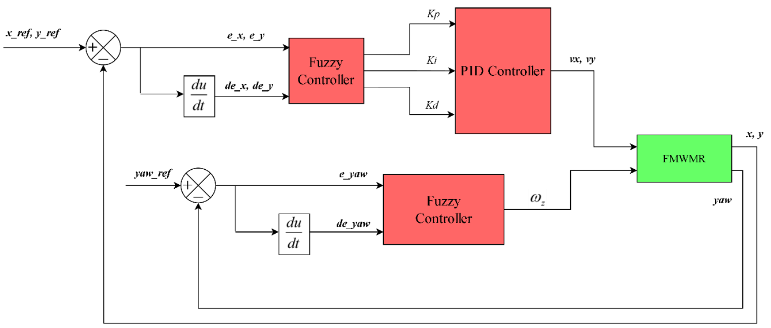

Figure 3. Block diagram of the control system

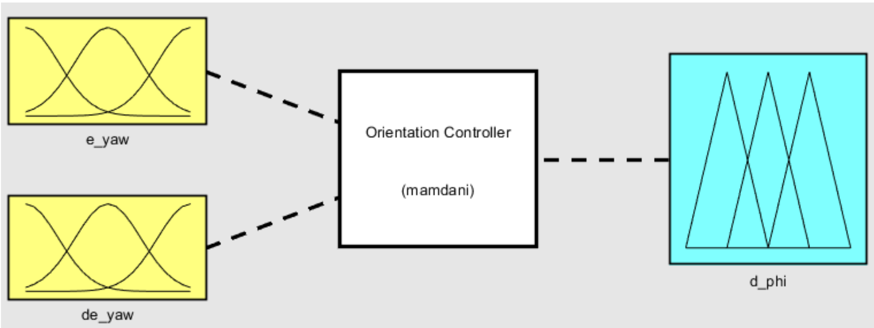

Figure 4. Inputs and output of heading angle Fuzzy logic controller

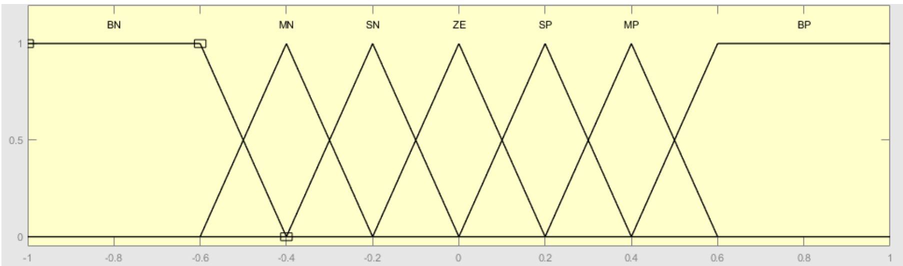

Figure 5. Design of membership functions for heading angle error's fuzzy input

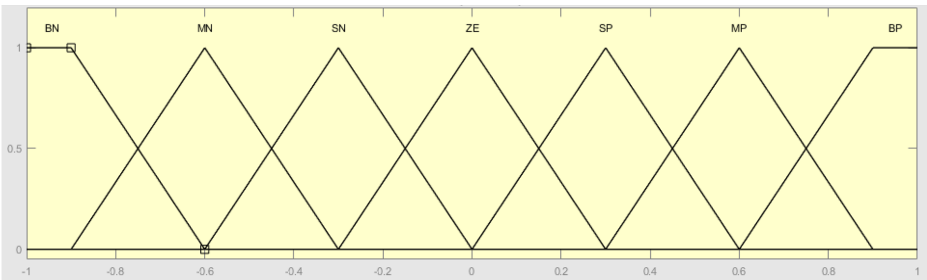

Figure 6. Design of membership functions for derivative of heading angle error fuzzy input

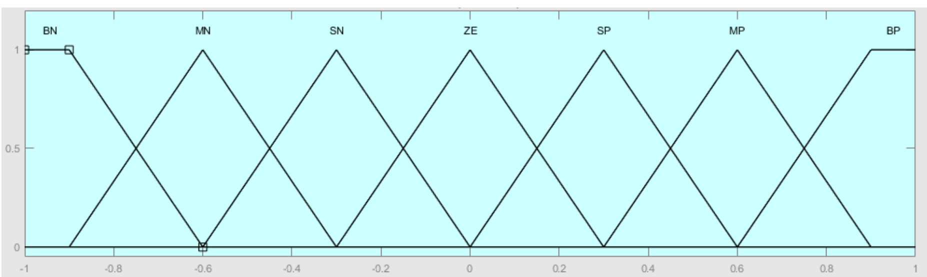

Figure 7. Design of membership functions for angular velocity fuzzy output

Table 1. Normalization gains of orientation fuzzy controller

Gain	Description	Value
K_{e-yaw}	Orientation error fuzzy input normalization gain	$1/\pi$
K_{de-yaw}	Orientation derivative of error fuzzy input normalization gain	$1/4\pi$
K_{ω}	Angular speed's fuzzy output normalization gain	$\pi/10$

Fuzzy Rule Base

The fuzzy rule base comprises a set of IF-THEN rules that determine the appropriate control action based on the linguistic values of the input variables. The rules consider the combination of error and rate of change of error to determine the appropriate velocities for the robot. Each rule specifies the linguistic values of the inputs and the desired linguistic value of the output. These fuzzy rules were derived from the experience of numerous simulations and experiments, aiming to achieve the most effective control system as shown in Table 2.

Fuzzy Inference System

Once the fuzzy rule base is established, the fuzzy inference system combines the fuzzy rules with the fuzzified input values to determine the appropriate control action. In this paper, the Mamdani's Fuzzy Inference method with Max–Min composition is applied. It involves combining the minimum of the degrees of membership for each rule during aggregation and considers the maximum value of these minimum values during defuzzification.

Defuzzification

The defuzzification process converts the fuzzy output into a crisp output value of the angular velocity. In this implementation, the Center of Gravity (COG) method is leveraged for defuzzification, which calculates the centroid of the aggregated output fuzzy set.

3.2. Fuzzy-PID controller for position control

This section presents the use of fuzzy logic to tune the parameters of PID controllers for trajectory tracking along the x and y axes. Two fuzzy PID controllers are independently designed for each axis. The structure of the fuzzy system, shown in Figure 8, includes two inputs (position error and its derivative) and three outputs (the PID controller gains). Similar to the orientation controller, all the inputs and outputs of fuzzy logic controller in this section are designed in a normalized range of [-1, 1] with inputs and [0, 1] with outputs. The details of the fuzzy tuning process are described as follows:

Table 2. Fuzzy rule base for heading angle control

ω_z		E						
		BN	MN	SN	ZE	SP	MP	BP
de	BN	BN	BN	BN	BN	MN	SN	ZE
	MN	BN	BN	MN	MN	SN	ZE	SP
	SN	BN	BN	SN	SN	ZE	SP	MP
	ZE	MN	MN	SN	ZE	SP	MP	MP
	SP	MN	SN	ZE	SP	SP	BP	BP
	MP	SN	ZE	SP	MP	MP	BP	BP
	BP	ZE	SP	MP	BP	BP	BP	BP

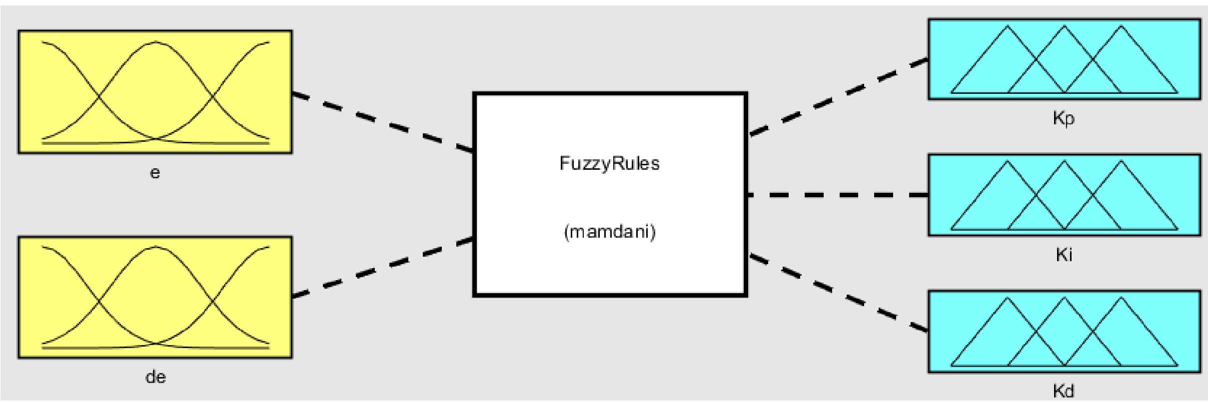

Figure 8. Structure of inputs and outputs Fuzzy logic design

For the inputs of fuzzy logic, each tracking position error along each axis ($e_x = x_r - x$ or $e_y - y_r - y$) is fuzzified using five membership functions: NB (Negative Big), NS (Negative Small), ZE (Zero), PS (Positive Small), and PB (Positive Big). Similarly, the derivative of the position tracking error (de_x or de_y) is fuzzified using the same five membership functions: NB (Negative Big), NS (Negative Small), ZE (Zero), PS (Positive Small), and PB (Positive Big). Figure 9 and Figure 10 illustrate the membership functions fuzzy logic inputs. The normalization gains are set to 0.02 for the position error and 0.04 for the error derivative.

The fuzzy outputs include three parameters of PID controller K_p, K_i and K_d, which are normalized in range of [0, 1]. These output values are fuzzified using five membership functions: S (Small), MS (Medium Small), M (Medium), MB (Medium Big), B (Big). The membership functions of these outputs are designed similarly as illustrated in Figure 11.

Based on the experience through extensive simulations and experiments, for best control performance, PID controller gains are chosen to vary in ranges of: K_p =[9, 11], K_i =[7, 12], K_d =[0.05, 1]. In fuzzy outputs, these parameters are normalized into the range of [0, 1] by equation (6).

$$K_x^{'} = \frac{K_x - K_{x\min}}{K_{x\max} - K_{x\min}} \tag{6}$$

where K_x stands for the reality PID gains K_p, K_i or K_d; and stands for the normalized PID gains (Fuzzy outputs) $K_p^{'}$, $K_i^{'}$ or $K_d^{'}$. From (6), the value of PID parameter gains can be calculated from fuzzy output by equation (7).

$$K_x = K_x^{'}(K_{x\max} - K_{x\min}) + K_{x\min} \tag{7}$$

Thus, as a result, the value of K_p, K_i or K_d can be detailed as: $K_p = 2K_p^{'} + 9$; $K_d = 0.05K_d^{'} + 0.05$; $K_i = 5K_i^{'} + 7$.

Based on tuning and evaluation of control of performance, the rule base for three outputs of the fuzzy logic is established in a similar manner and is illustrated as in Table 3.

To determine the fuzzy outputs, the Mamdani Fuzzy Inference Method with Max–Min composition and COG defuzzification, is applied. This method is identical to the design process used for the fuzzy controller in orientation control mentioned earlier.

4. Experiential Setup and Heading Angle Fusion Technique

4.1. Experimental Setup

The structure of the experimental control system is illustrated in Figure 12. In this setup, the vision-based ArUco marker detection method and trajectory tracking Fuzzy PID controllers are executed on a laptop computer. The ATmega 2560 is responsible

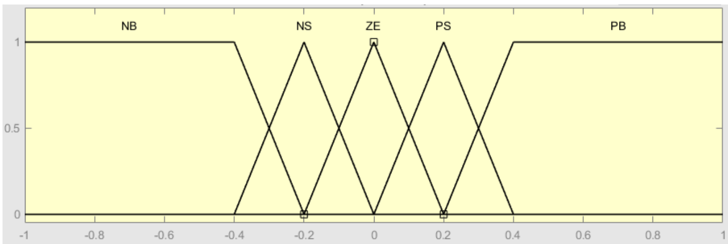

Figure 9. Position error's membership function

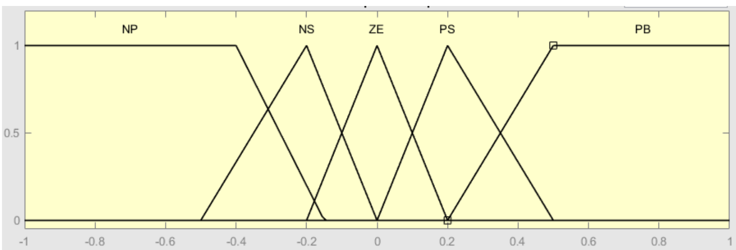

Figure 10. Derivative of position error's membership function

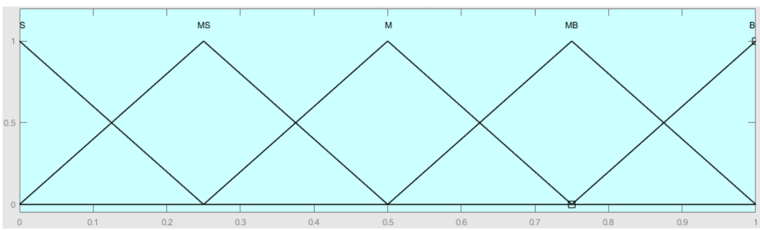

Figure 11. Membership function for fuzzy outputs - the PID normalized gains $K_p^{'}$, $K_i^{'}$, $K_d^{'}$

for calculating the robot's orientation (Magdwick and Complementary filters), executing the heading angle Fuzzy controller, and managing the wheel speed PID controllers. Communication between the laptop and the ATmega 2560 is facilitated via a Bluetooth module (HC-05). The block diagram showing the functional blocks of the real-world implementation for mecanum robot control is presented in Figure 13.

4.2. Heading Fusion Technique

Accurate heading angle estimation is crucial for precise trajectory tracking and motion control in FMWMRs. To achieve reliable and robust heading angle estimates, a sensor fusion approach that combines data from a camera-based localization system and an Inertial Measurement Unit (IMU) is investigated.

Table 3. Fuzzy rule base for controlling K_P, K_I, K_D

K_x'		e				
		NB	NS	ZE	PS	PB
de	NB	B	MB	S	S	M
	NS	B	M	S	MS	MB
	ZE	MB	MS	S	MS	MB
	PS	MB	MS	S	M	B
	PB	M	S	S	MB	B

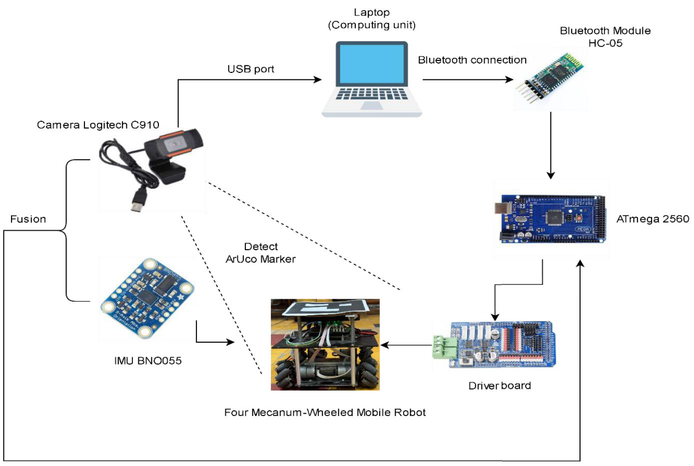

Figure 12. Structure of the experimental execution

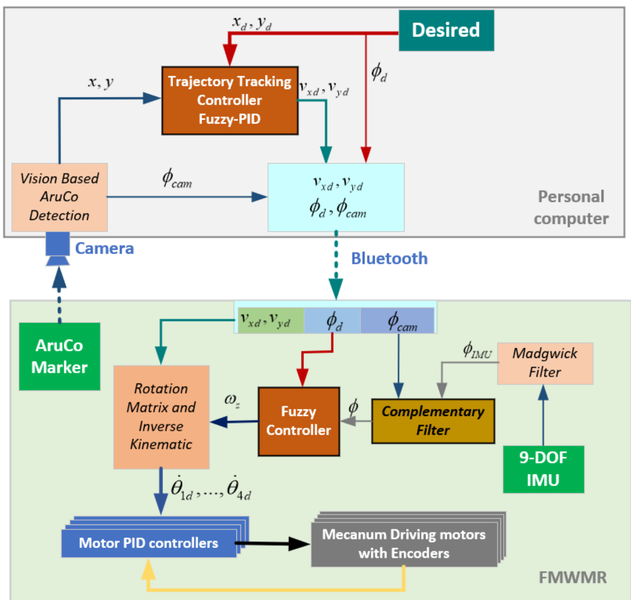

Figure 13. Overall block diagram of real-life FMWMR control

An ArUco marker affixed to the robot is detected by the camera-based localization system, employing an overhead camera. Through analysis of the marker's pose, the system establishes the robot's position and orientation in the global coordinate system. Despite its utility, ArUco marker detection is susceptible to limitations such as sensitivity to lighting conditions and a slow detection… To mitigate these constraints, IMU data are concurrently utilized to augment the accuracy of heading angle detection. The IMU integrates signals from accelerometers, magnetometers, and gyroscopes, facilitating the Madgwick filter [44] in estimating a drift-free and responsive heading angle. Subsequently, the robot's heading angle is determined by combining data from both the camera and IMU using the complementary filter [43]. Here, the IMU supplies rapid angle variations via a high-pass filter, complemented by the camera's provision of slower variations through a low-pass filter. Figure 14 illustrates the complementary filter integration.

The mathematical models of the complementary filter using first order filter in both Laplace and Z domains are expressed in Eq. (8) and (9), respectively.

$$\phi_{fused}(s)=\frac{\tau s}{\tau s+1}\phi_{IMU}(s)+\frac{1}{\tau s+1}\phi_{cam}(s) \tag{8}$$

$$\phi_{fused}(z)=\frac{1-z^{-1}}{1-\alpha z^{-1}}\phi_{IMU}(z)+\frac{(1-\alpha)z^{-1}}{1-\alpha z^{-1}}\phi_{cam}(z) \tag{9}$$

Consequently, the final heading angle can be computed from the IMU and camera as equation (10).

$$\phi_{fused}(k)=\alpha\phi_{fused}(k-1)+[\phi_{IMU}(k)-\phi_{IMU}(k-1)]+(1-\alpha)\phi_{cam}(k-1) \tag{10}$$

where: ϕ_{fused} is fused heading angle (degree); ϕ_{cam} is heading angle from the camera (degree); ϕ_{IMU} is heading angle from the IMU (degree); $\alpha=e^{-T_s/\tau}$; T_s is sampling time; τ is low-pass filter time constant which is chosen as 1s in this research.

Figure 15 presents a comparison of the IMU response, vision detection, and the fusion results. Figure 15a highlights the IMU response obtained from Magdwick filter, showing significant detection errors due to accumulation effects and environmental uncertainties. In contrast, Figure 15b displays the vision detection result from the Aruco marker. This result is shown under the worst conditions, where light variability and pixel errors heavily impact detection accuracy. Finally, Figure 15c illustrates the outcome of the complementary filter. This fusion response demonstrates the advantages of the fusion method, effectively reducing the drawbacks of both the IMU and vision sensors. The enhanced heading angle from the fusion can be applied to experimental control in further sections.

5. Results and Discussion

To evaluate the performance of the proposed control system and sensor fusion approach, extensive simulations and real-world experiments are conducted. This section presents and analyzes the results obtained from both the simulation studies and the experimental validation.

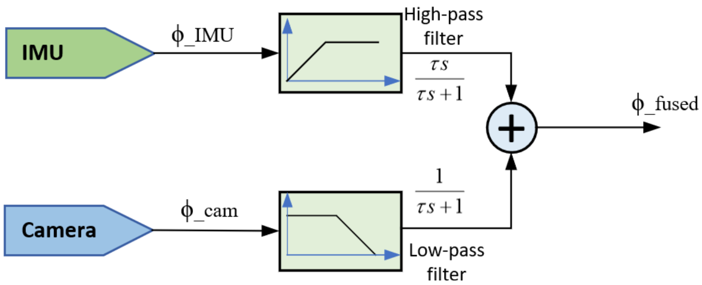

Figure 14. Block diagram of heading angle fusion using complementary filter

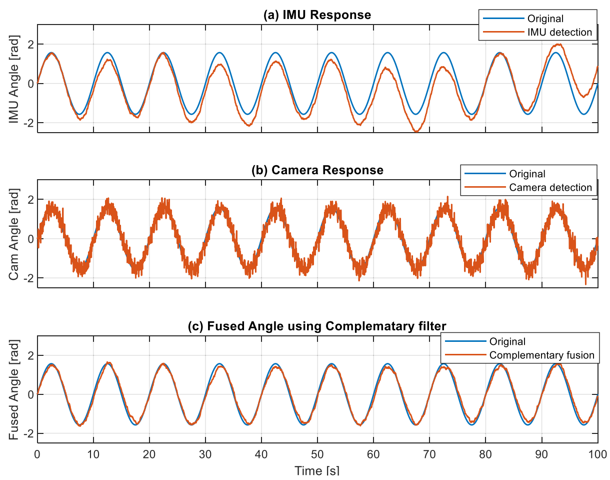

Figure 15. Heading angle detection using IMU, Vision- ArUco marker and Complementary filter fusion

5.1. Simulation Results

Simulation results using Matlab/Simulink environment are performed to compare the tracking performance of three control strategies: PID, Fuzzy, and Fuzzy-PID. The simulations were carried out under various scenarios, including desired position, rectangular reference trajectory and eight-shaped reference trajectory.

For the desired position scenario, the response and error plots are illustrated in Figure 16 and Figure 17, respectively. Analysis of the response plots demonstrates that the Fuzzy controller achieves the fastest response in reaching the desired x and y positions. In comparison, the PID controller responds slightly slower and exhibits some oscillation before settling while both Fuzzy and Fuzzy-PID controllers show quick and smooth convergence to the desired yaw angle. Despite the differences in response times, all three controllers successfully converge to the target position and heading angle with minimal steady-state error.

Next, the rectangular path trajectory scenario control results are presented in Figure 18 to Figure 20, respectively. From the robot's path in the x-y plane, it is obvious that the Fuzzy-PID controller performs the best, attaining the smoothest and most accurate tracking (Figure 18). The Fuzzy-PID controller maintains the lowest error values in all dimensions (x, y, and heading angle), as shown by the error plots (Figure 20), which validate its improved tracking accuracy. Though having somewhat greater deviations and error magnitudes than the Fuzzy-PID controller, the fuzzy controller also shows good tracking capabilities. On the other hand, the tracking performance of the PID controller is less accurate, exhibiting more pronounced oscillations, undershoots, and overshoots, especially at the rectangle's corners.

Besides, an eight-shaped trajectory was utilized to assess the controllers' performance further in Figure 21 to Figure 23. This difficult maneuver tests the robot's capacity to manage abrupt direction changes and sharp turns. All three controllers are able to follow the intended

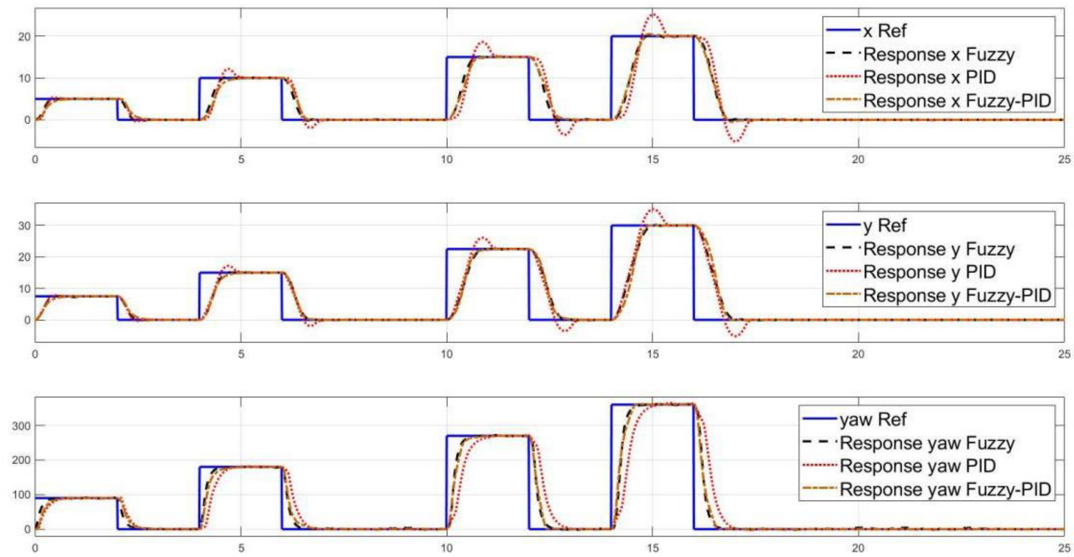

Figure 16. Position responses with respect to multi-step reference in simulation

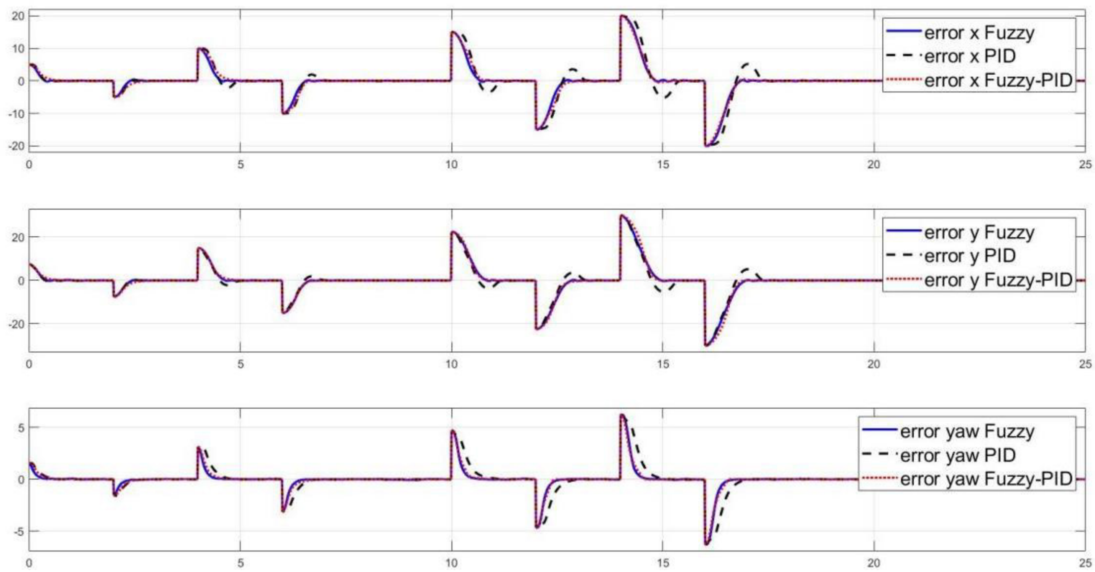

Figure 17. Position control errors with respect to multi-step reference in simulation

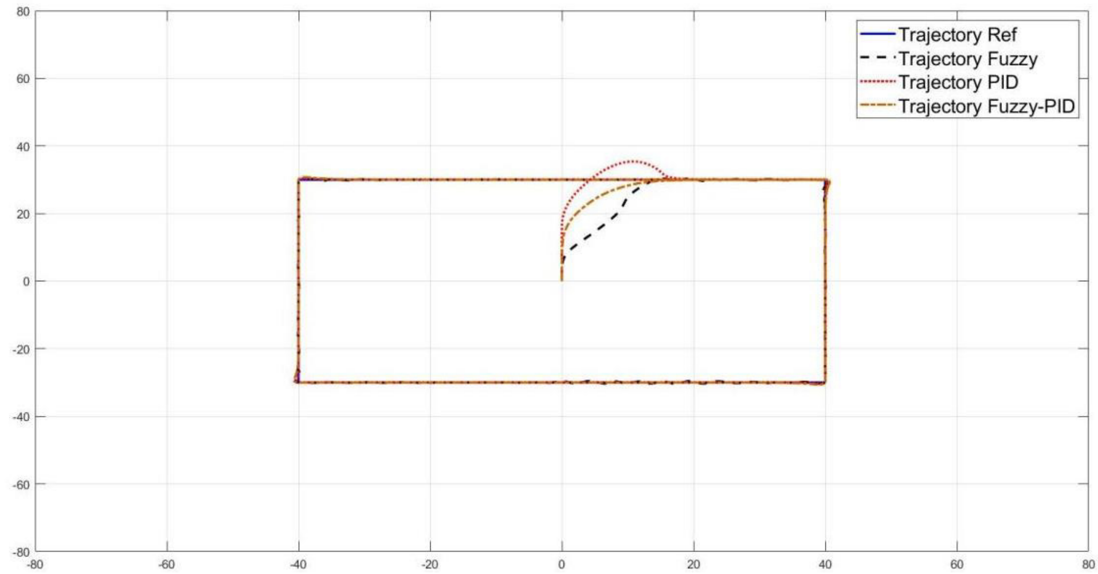

Figure 18. Rectangular path trajectory tracking control responses in simulation

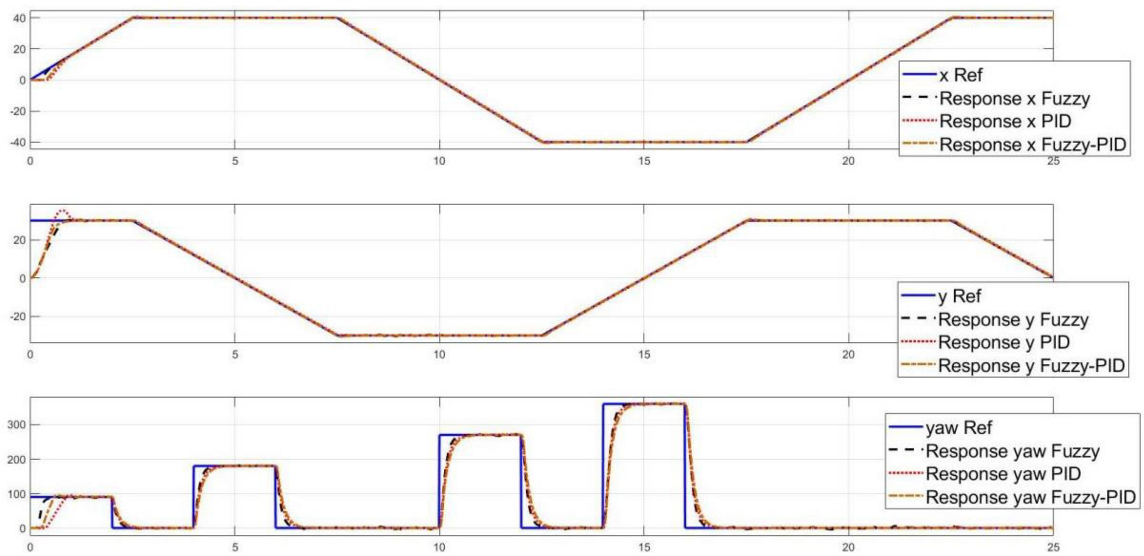

Figure 19. Control responses with respect to rectangular path trajectory tracking control in simulation

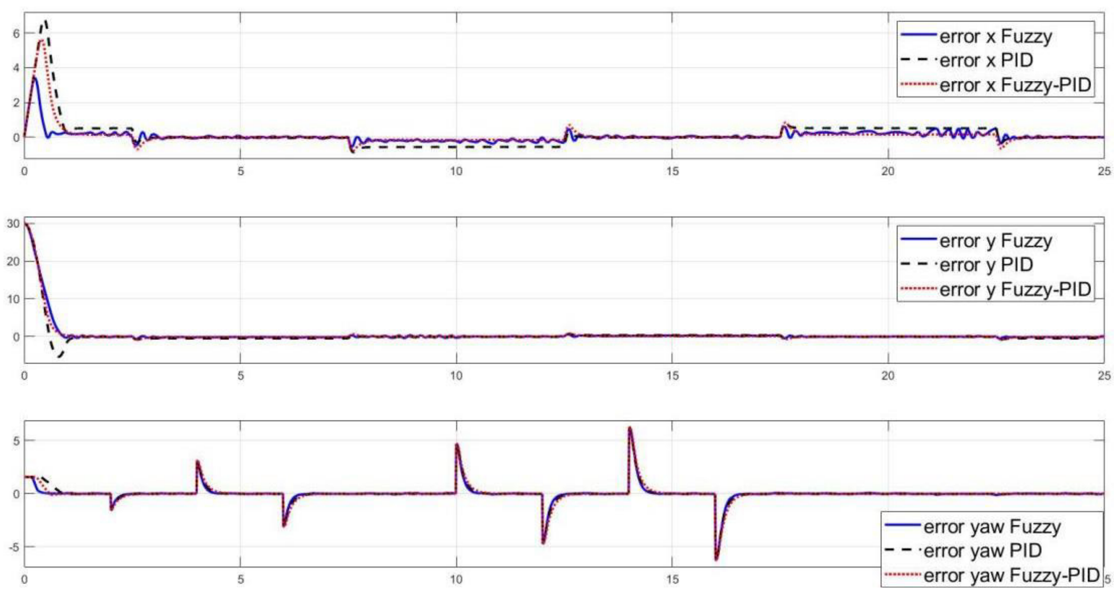

Figure 20. Control errors with respect to rectangular path trajectory tracking control in simulation

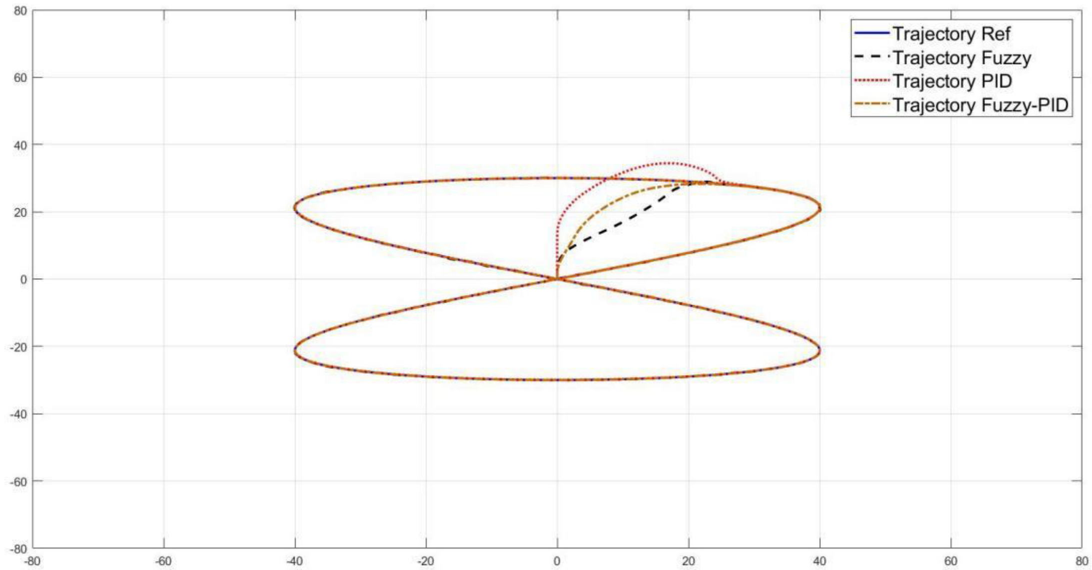

Figure 21. 8-shaped path trajectory tracking control results in simulation

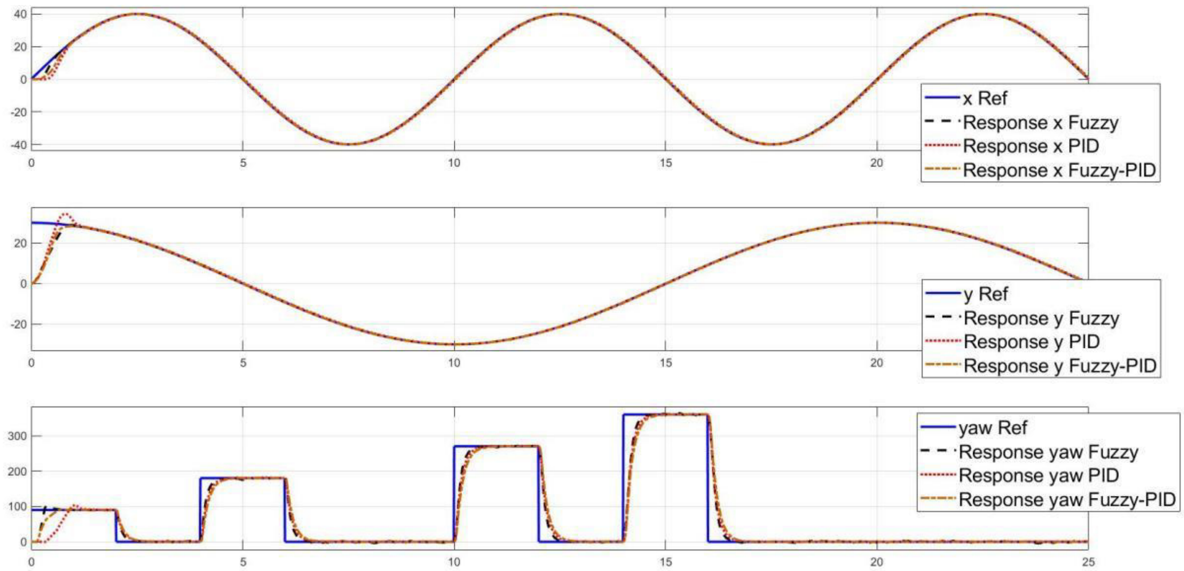

Figure 22. Control responses with respect to 8-shape path trajectory tracking control in simulation

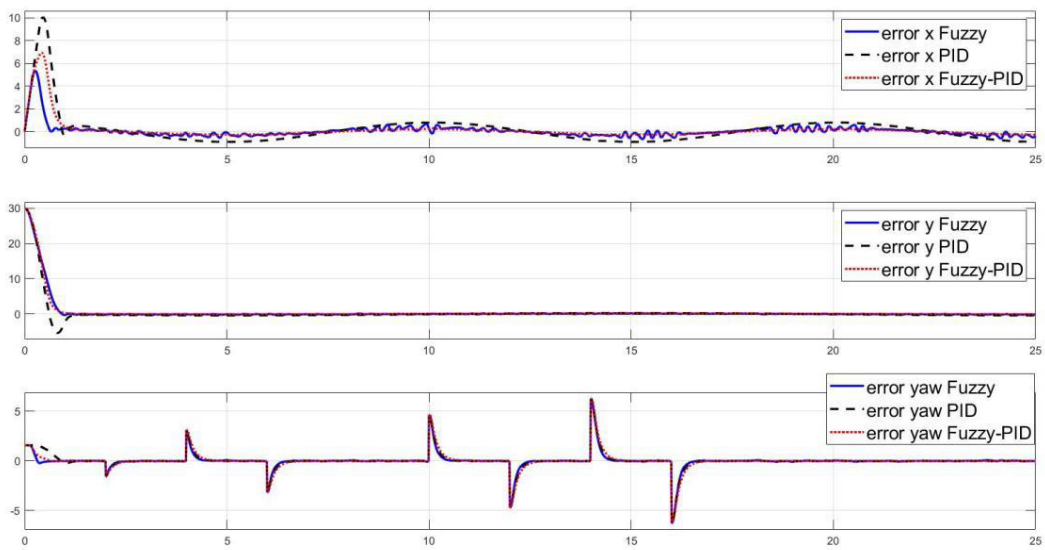

Figure 23. Control response error with respect to 8-shape path trajectory tracking control in simulation

8-shaped path, as seen by the trajectory tracking plot (Figure 21), with the Fuzzy-PID controller adhering to the reference trajectory that is closest. The Fuzzy-PID controller outperforms the others, as seen by the error plots (Figure 23), which show the lowest x, y, and heading angle error magnitudes. Whereas the PID controller displays greater error magnitudes, the fuzzy controller maintains very low error values.

Based on simulation results, the control performances of three controllers are evaluated. Table 4 and table 5 present the comparison results of these controllers. These tables display each controller's x-position and yaw responses across four criteria: Overshoot, rise time, steady-state error, and settling time. The results demonstrate that the Fuzzy-PID controller exhibits superior performance, characterized

Table 4. Comparison among the x responses of each controllers

Setpoint	Parameters	PID	Fuzzy	Fuzzy-PID
5	Overshoot (%)	8.02	5.07	0
	Rise time (s)	0.31	0.24	0.37
	Steady state error	0.0273	0.0089	0
	Settling time (s)	0.63	0.5	0.77
10	Overshoot (%)	21.8	1.43	0
	Rise time (s)	0.26	0.34	0.44
	Steady state error	0.0318	0.006	0
	Settling time (s)	1.01	0.55	0.87
15	Overshoot (%)	24.07	2.09	0
	Rise time (s)	0.31	0.22	0.47
	Steady state error	0.0585	0.0007	0
	Settling time (s)	1.19	0.66	0.74
20	Overshoot (%)	26.05	0.8	2.05
	Rise time (s)	0.35	0.48	0.51
	Steady state error	0.0722	0.0002	0.0002
	Settling time (s)	1.36	0.81	0.79

Table 5. Comparison among the yaw responses of each controllers

Setpoint	Parameters	PID	Fuzzy	Fuzzy-PID
90	Overshoot (%)	1.24	1.11	0.06
	Rise time (s)	0.39	0.25	0.33
	Steady state error	0.2911	1.23	0.07
	Settling time (s)	0.93	0.61	0.69
180	Overshoot (%)	0.55	0.27	0
	Rise time (s)	0.4	0.26	0.34
	Steady state error	1.167	0.386	0.32
	Settling time (s)	0.78	0.48	0.72
270	Overshoot (%)	0.4	0.39	0
	Rise time (s)	0.52	0.25	0.31
	Steady state error	1.48	0.756	0.126
	Settling time (s)	1	0.55	0.63
360	Overshoot (%)	1.2	0.03	0
	Rise time (s)	0.54	0.27	0.37
	Steady state error	2.76	1.35	0.57
	Settling time (s)	0.94	0.56	0.54

by zero overshoot, minimal steady-state error, and a fast response.

Overall, the Fuzzy-PID controller has the best overall performance for both the x and yaw responses, offering exceptional stability, precision, and convergence speed, according to the provided data. The Fuzzy controller is a dependable option since it provides a decent balance between stability and responsiveness. With greater overshoot, slower response times, and larger steady-state errors than the other two controllers, the PID controller performs less well than the other two. From the obtained simulation results, we proposed a novel control approach for the FMWMR model in a real-life system. The experimental results will be discussed in detail in the following section.

5.2. Experimental Results

The superior performance of the Fuzzy PID controller is demonstrated by the simulation results. In this subsection, this controller will be employed and experimental results will be presented under various conditions. The performance of the control system will be investigated in different scenarios, including desired position, elliptical trajectory, rectangular trajectory, circular trajectory, and eight-shaped path trajectory. Furthermore, the robustness and tracking quality of the controller will be verified under a loaded condition of 2.5 kg. The examination of the control system's tracking accuracy and path-following capability will be prioritized, with the unloaded condition applied specifically to the evaluation of the circular trajectory and eight-shaped path trajectory scenarios.

5.2.1. Desired position control scenario

In this experiment, the robot is set to move to the target position with coordinates x = 30cm, y = 30cm, and a yaw angle of 60 degrees. The control results are illustrated in Figure 24 to Figure 27. Figure 24 depicts the robot's positional response in terms of x

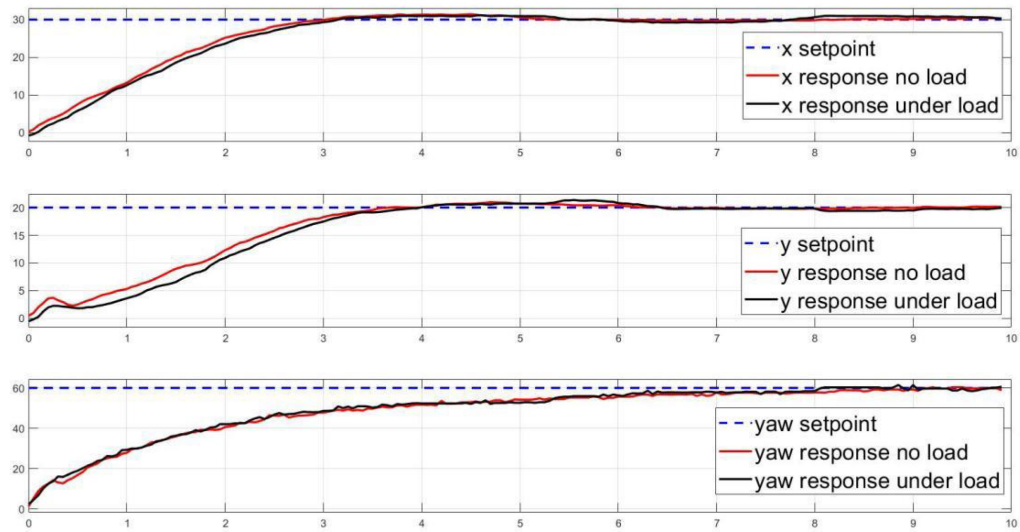

Figure 24. Responses of robot with respect to target setpoint

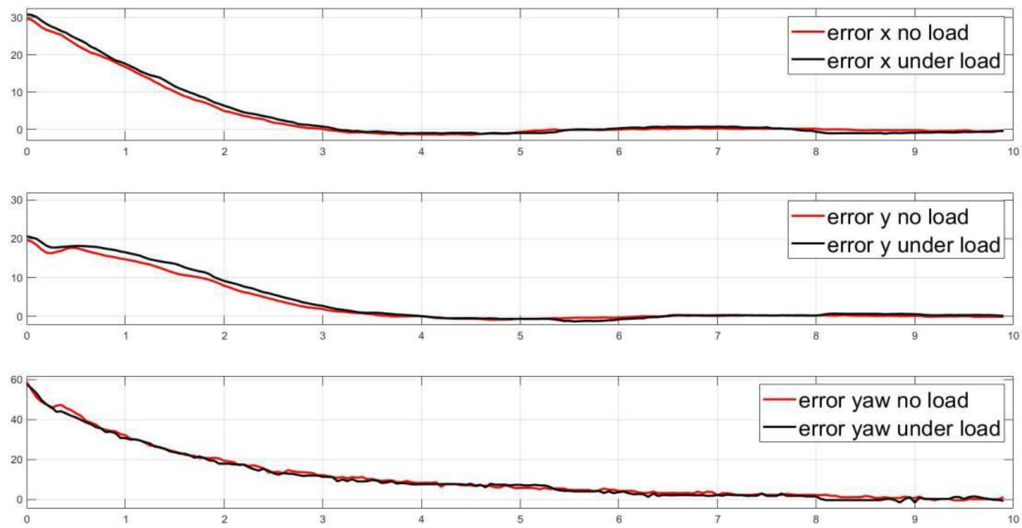

Figure 25. Errors of robot with respect to target setpoint

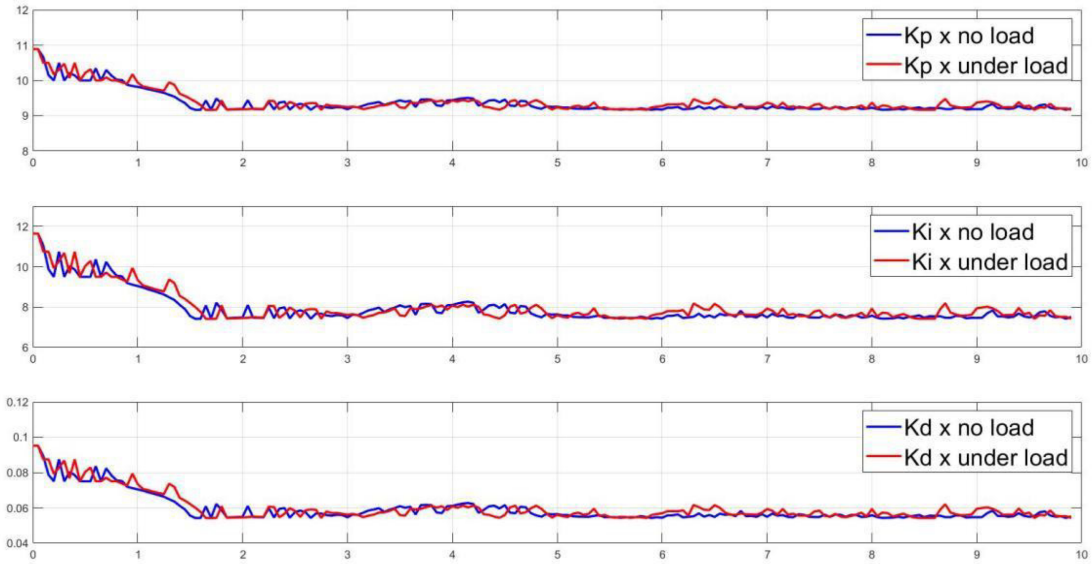

Figure 26. PID Gains tuning results with respect target setpoint in x-dimension

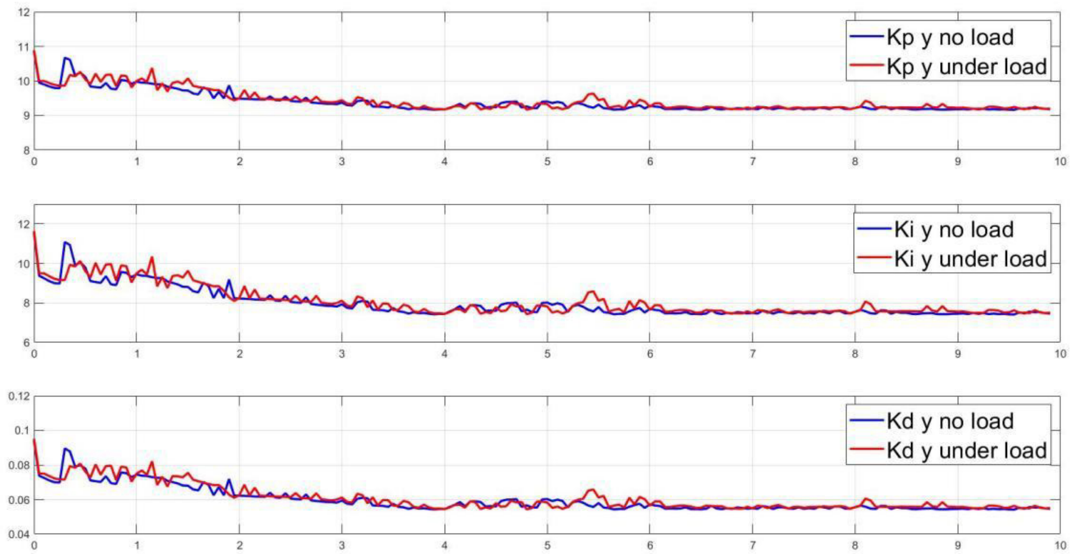

Figure 27. PID Gains tuning results with respect to target setpoint y-dimension

and y coordinates as well as yaw angle. It is evident that the robot reaches the target position within three seconds without any overshoot, while the yaw angle takes six seconds to stabilize. The steady-state error is nearly zero. The gains of the PID controllers are adjusted online and visualized in Figure 26 and Figure 27. Additionally, the effect of a 2.5kg load is examined in this scenario, revealing that the designed controller can adapt effectively to changes in load. The control performance remains consistent with that of the unloaded condition.

5.2.2. Elliptical trajectory tracking control scenario

The designed controller is then put to the test to guide the robot in tracking an elliptical trajectory. The elliptical path is configured to be 50cm long and 30cm wide along the x-y directions, with a heading angle set at -45 degrees. The results of this control experiment are presented in Figure 28 through Figure 32. Figure 28 illustrates the tracking performance within the x-y plane, showcasing effective trajectory tracking with minimal error. Detailed control responses for the x, y positions, and yaw angle are depicted in Figure 30, demonstrating consistent performance comparable to the initial scenario. Additionally, the tuning results for the PID controllers are visualized in Figure 31 and Figure 32.

5.2.3. Rectangular trajectory scenario

The final case examined under two loading conditions involves tracking a rectangular trajectory. In this experiment, the robot is configured to follow a rectangular path with dimensions of 80 cm in length along the x-direction and 60 cm in width along the y-direction, with a desired yaw angle set at 20 degrees. The control results are presented in

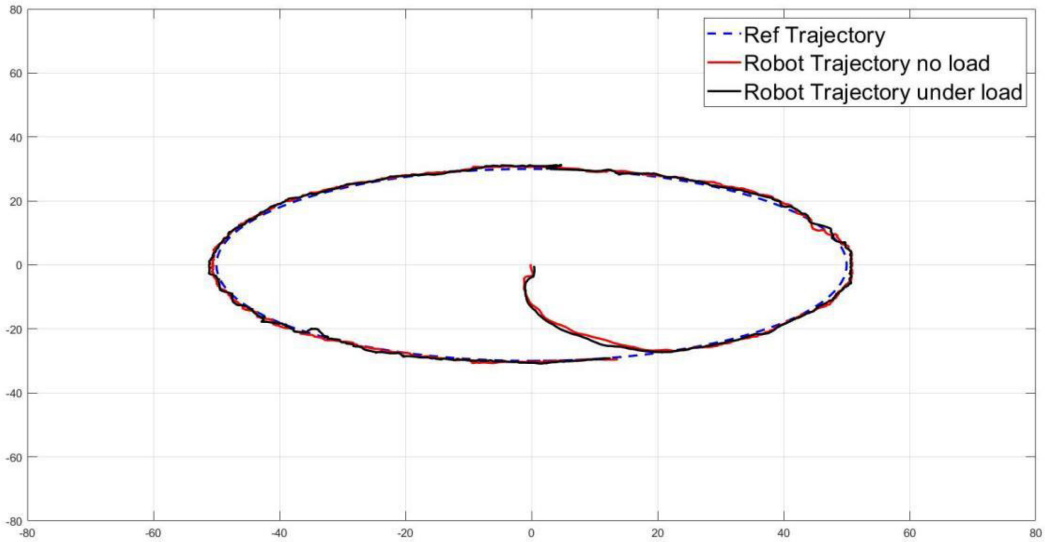

Figure 28. Trajectory tracking responses with respect to elliptical trajectory in x-y plant

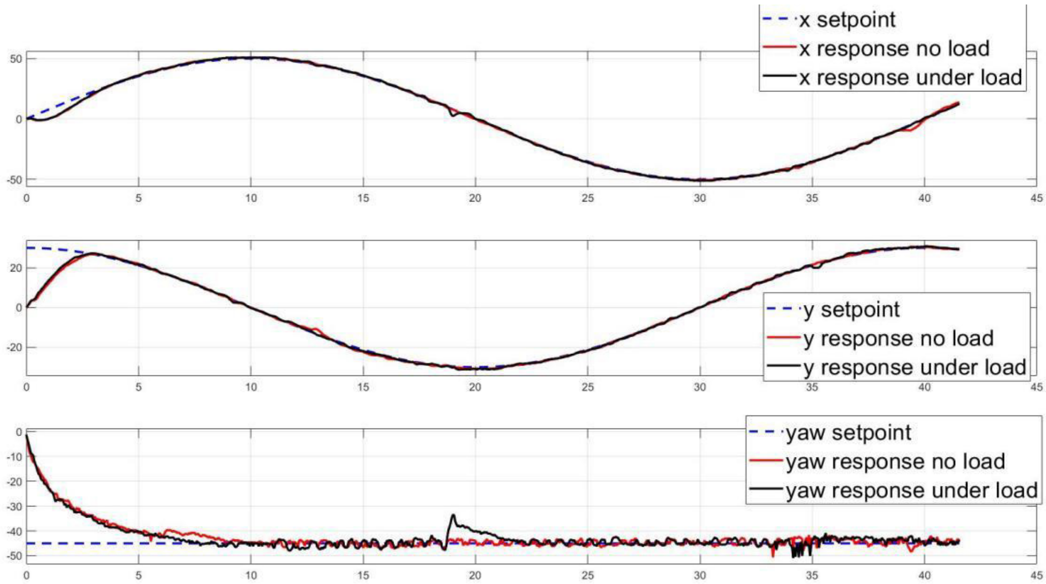

Figure 29. Robot position responses with respect to elliptical trajectory

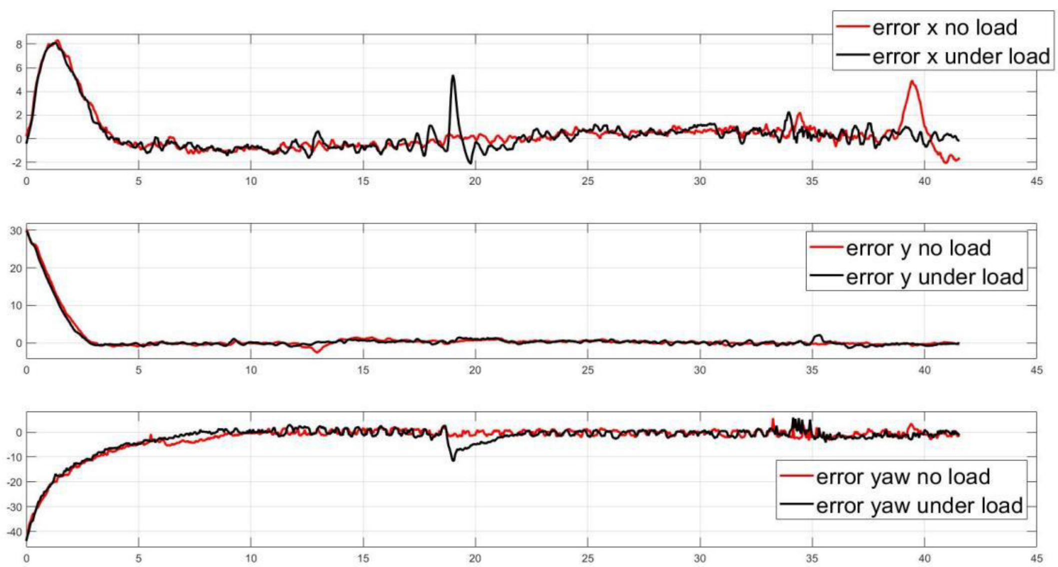

Figure 30. Robot position tracking errors with respect to elliptical trajectory

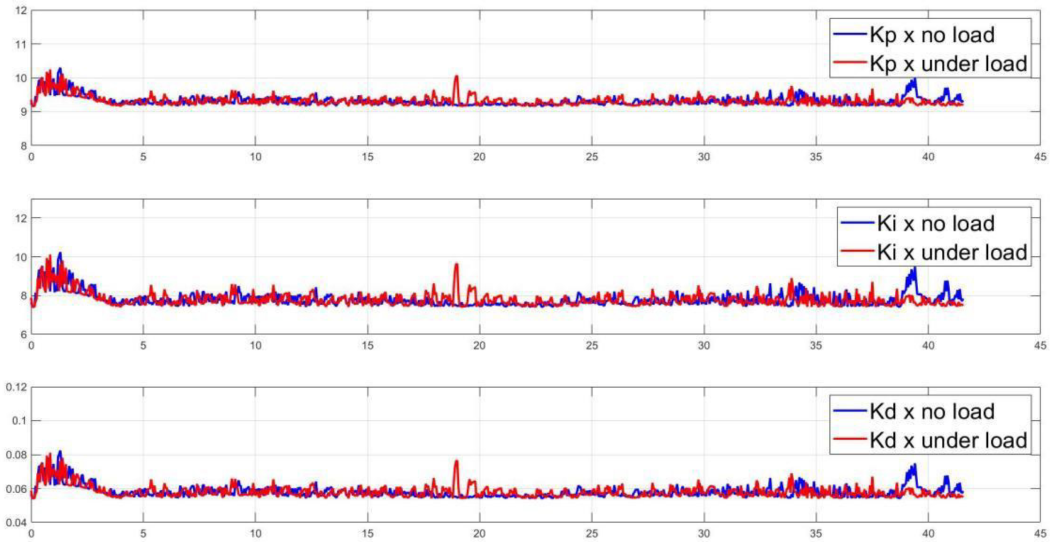

Figure 31. PID gains tuning results with respect to elliptical trajectory in x dimension

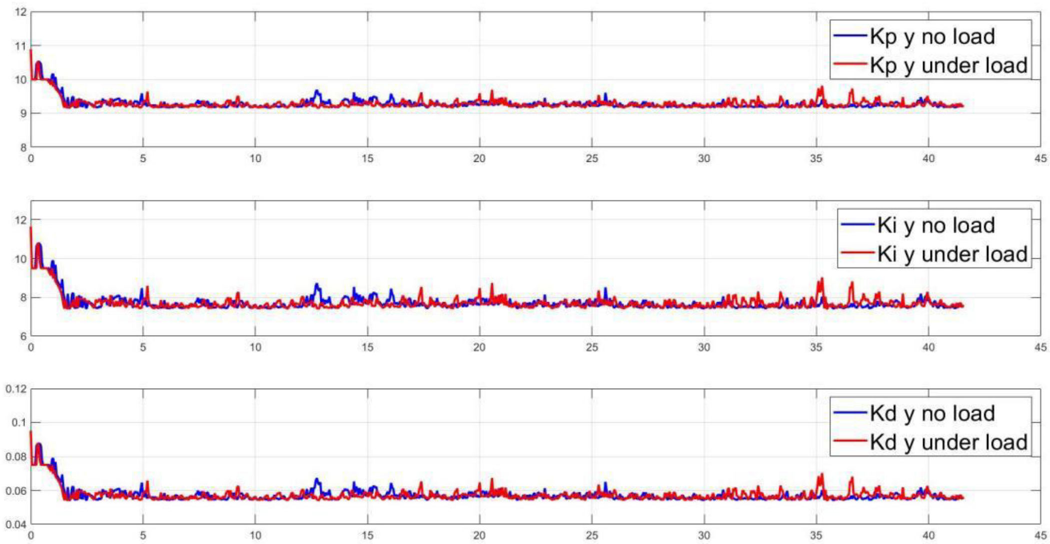

Figure 32. PID gains tuning results with respect to elliptical trajectory in y dimension

Figure 33 rough Figure 35. These results demonstrate that the controller effectively guides the robot to track the desired trajectory, exhibiting minimal steady-state error and low overshoot. It's notable that in this scenario, there is some overshoot due to sudden changes in the desired x-y direction, causing the robot, with its inertia, to continue moving in a certain direction.

In summary, to quantitatively assess the performance of the control system, the root mean square error (RMSE) values in the x, y, and yaw dimensions are calculated. Table 6 displays the RMSE values for different scenarios under both unload and load conditions. From the RMSE table, it is observed that the RMSE values for x and y dimensions in rectangular trajectory tracking are the largest, attributed to sudden changes in the desired trajectory. However, the RMSE values under load conditions do not show significant differences. This indicates that the designed controller effectively handles load conditions.

5.2.4. Circular trajectory and eight-shape trajectory scenarios

Moreover, the designed controller is evaluated for its ability to guide the robot along circular and eight-shaped trajectories. The control outcomes are illustrated in Figure 36 through Figure 41. Figure 36 to Figure 38 depict the tracking control results for the circular trajectory, while Figure 39 to Figure 41 display the results for the eight-shaped trajectory. Consistent with previous scenarios, the robot adeptly follows the circular path with commendable accuracy, maintaining a consistent shape throughout the trajectory. Overall, across various scenarios, the controller exhibits consistent performance and robustness, demonstrating its ability to adapt to different trajectories and load conditions.

5.3. Discussion

The accuracy and robustness of the Fuzzy-PID controller for four wheels mecanum robot trajectory

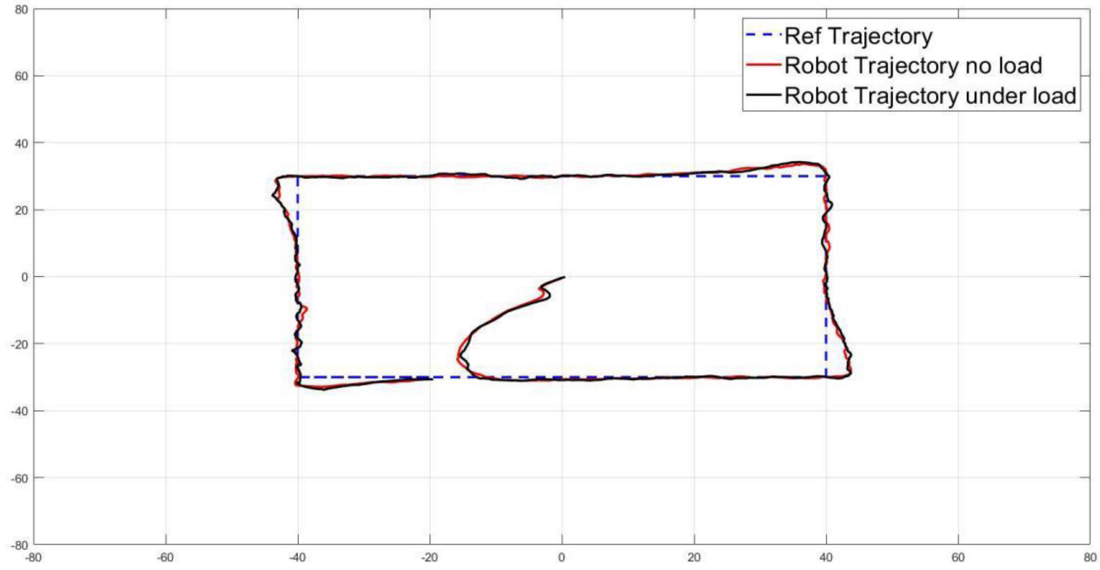

Figure 33. Trajectory tracking responses with respect to rectangular trajectory in x-y plant

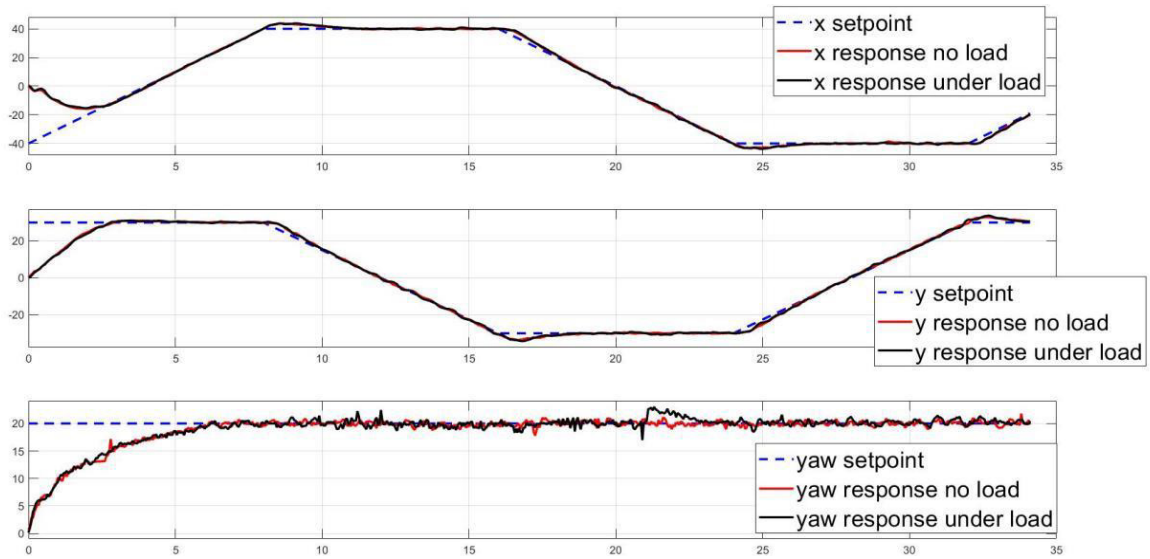

Figure 34. Robot position responses with respect to rectangular trajectory

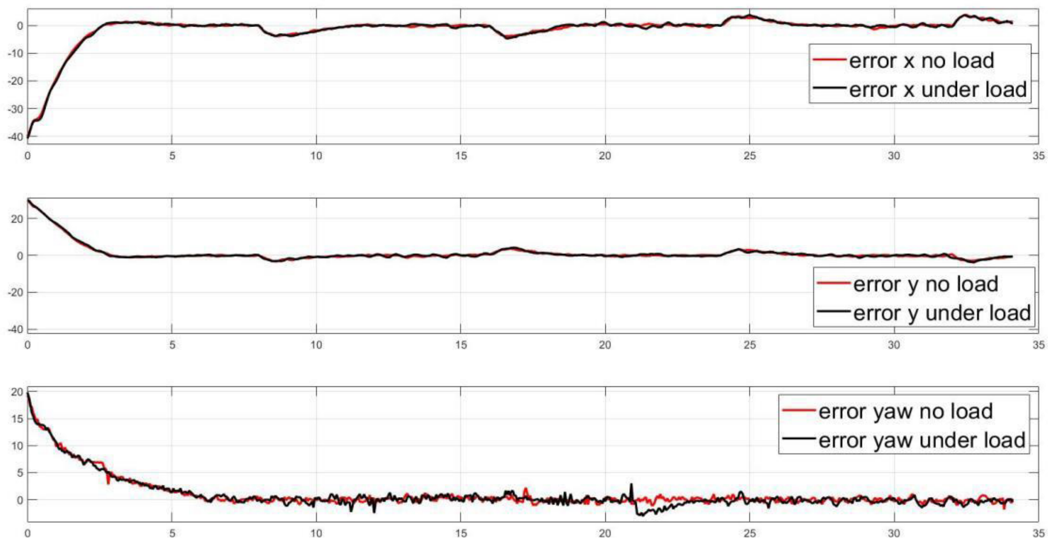

Figure 35. Robot position tracking errors with respect to rectangular trajectory

Table 6. RMSE values of tracking error

RMSE value	Target Setpoint		Elliptical Trajectory		Rectangular Trajectory	
	Without Load	With Load	Without Load	With Load	Without Load	With Load
$e_{x_{RMS}}$ (cm)	0.5859	0.7273	0.9443	0.8152	1.4152	1.421
$e_{y_{RMS}}$ (cm)	0.3483	0.5684	0.5421	0.5366	1.1642	1.1629
$e_{yaw_{RMS}}$ (degree)	1.583	1.8294	1.163	2.0261	0.4476	0.7072

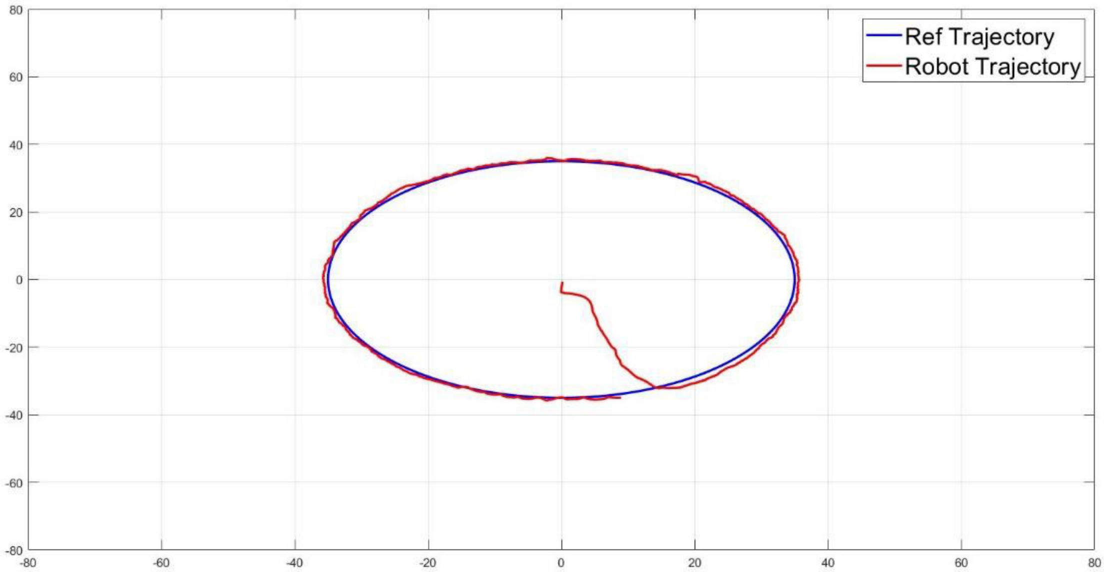

Figure 36. Trajectory tracking response with respect to circular trajectory in x-y plant

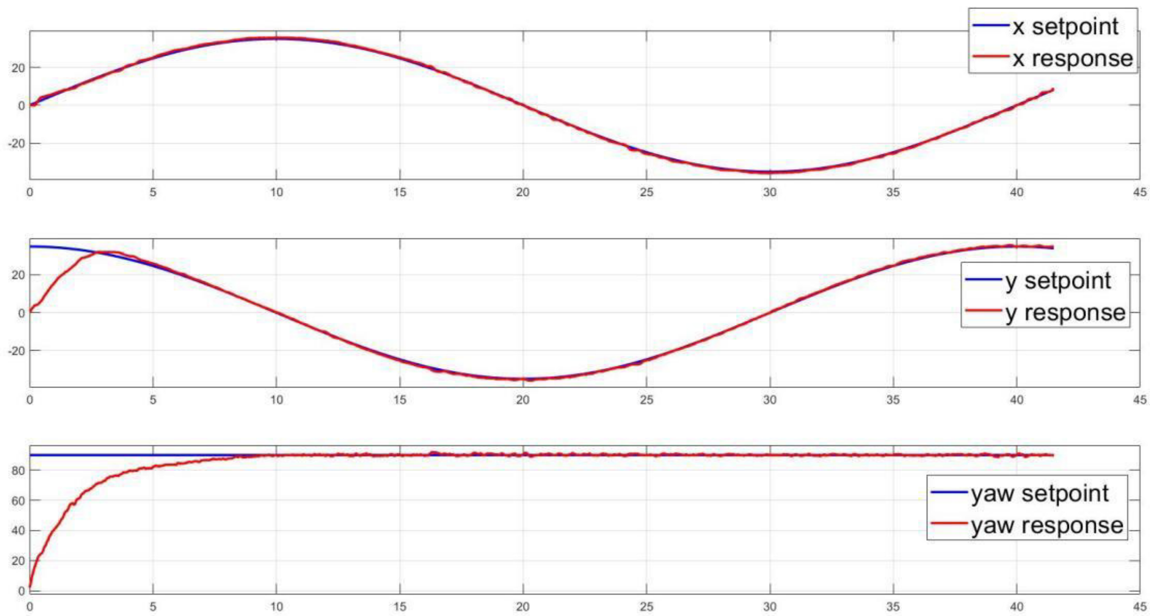

Figure 37. x-y positions and yaw angle tracking control responses with respect to circular trajectory

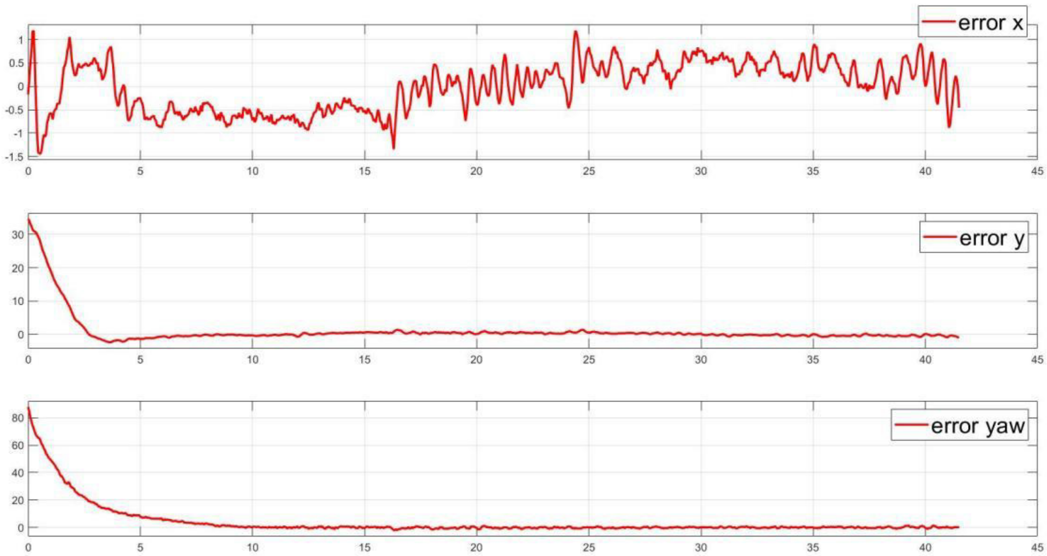

Figure 38. Tracking errors with respect to circular trajectory

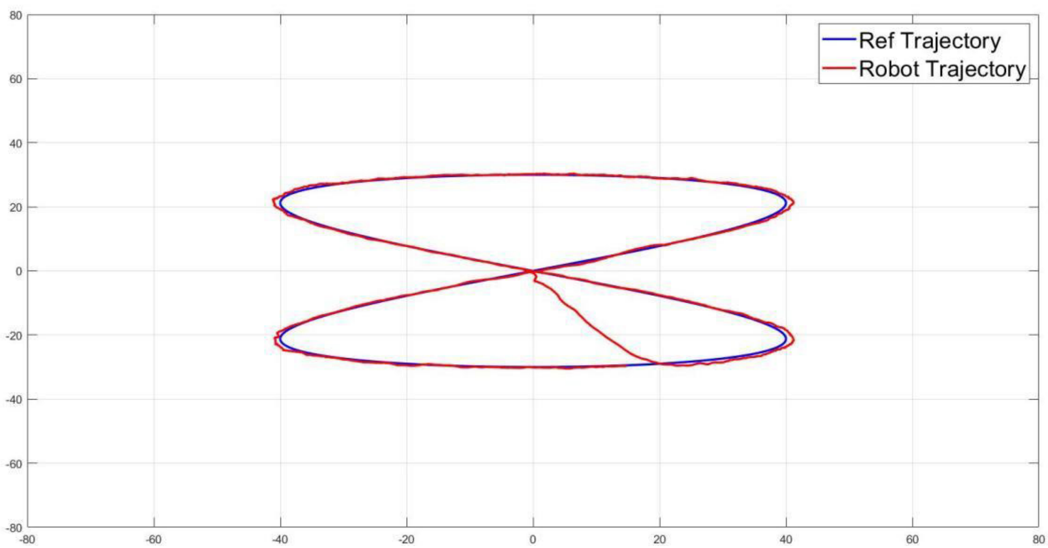

Figure 39. Trajectory tracking response with respect to eight-shape trajectory in x-y plant

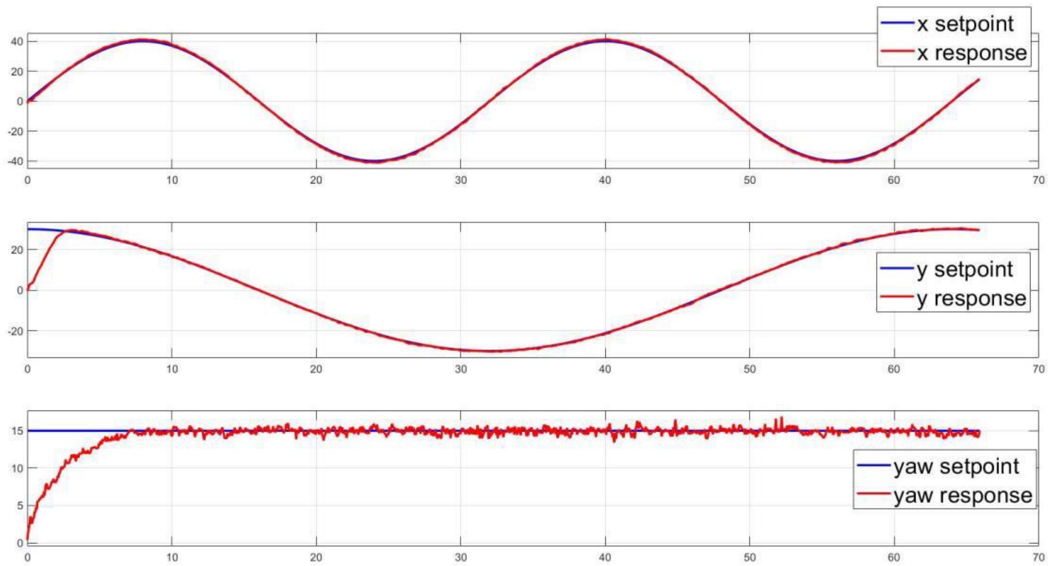

Figure 40. x-y positions and yaw angle tracking control with respect to eight-shape trajectory

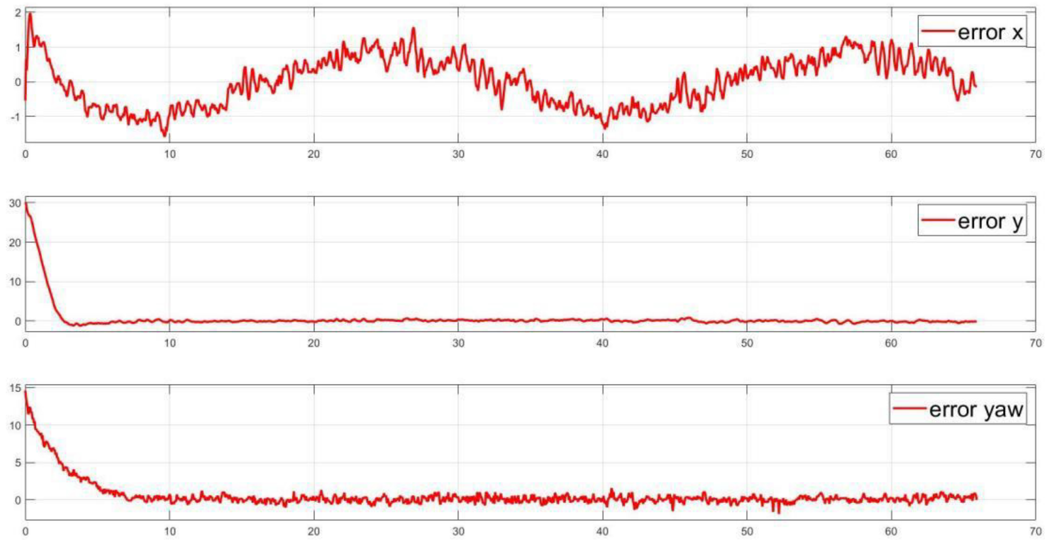

Figure 41. Tracking errors with respect to eight-shape trajectory

tracking under numerous scenarios and loading conditions are shown by the simulation and experimental results reported in this paper. The results of the simulation demonstrate that when it comes to providing accurate and smooth tracking of complex trajectories, the fuzzy-PID controller outperforms the PID and fuzzy controllers. The ability of the Fuzzy-PID controller to combine the advantages of fuzzy logic with PID control accounts for its higher tracking accuracy when compared to the standalone Fuzzy and PID controllers.

The proposed control system's performance in different trajectories, including desired position, elliptical, rectangular, circular, and eight-shaped path, is further validated by the experimental results. Excellent tracking precision, resilience, and adaptability are demonstrated by the control system in both loading conditions. Plots for trajectory tracking, response, error, and PID gain reveal the system's capacity to maintain accurate tracking, stable performance, and smooth motion even when additional payloads are present.

A quantitative assessment of the tracking accuracy of the control system and the effect of the load on its operation is given by the RMSE analysis. The findings demonstrate that, despite a slight decrease in tracking accuracy brought about by the increased load, the control system is still able to maintain comparatively low RMSE values, guaranteeing accurate trajectory tracking and positional control. The load has varying effects on the different dimensions; the y-dimension is most affected, followed by the x- and yaw-dimensions. For mobile robots to be implemented in a variety of industrial and service sectors where payload weight frequently varies, the control system must be able to maintain consistent performance under changing load situations.

6. Conclusion

In this paper, a novel control approach of combining a Fuzzy-PID controller for position control and a Fuzzy controller for heading control has been proposed and investigated for the FMWMR. Moreover, a sensor fusion technique, which combines data from the camera and IMU, is also implemented for enhancing heading angle estimation. The control system's outstanding performance in providing precise and smooth tracking of various trajectories under different loading cases has been proved by the results of simulations and experiments. Because of its versatility and resilience while managing changes in payload, the system has great promise for the real-world implementation of mobile robots in industrial and service applications. Our research's finding advances the development of mobile robot control algorithms by leveraging the benefits provided by multi-sensor data fusion technique.

List of abbreviations

FMWMR: Four Mecanum-Wheeled Mobile Robots
PID: Proportional Integral Derivative
GPS: Global Positioning System
IMU: Inertial Measurement Unit
COG: Center Of Gravity

Declarations

Availability of data and materials The authors confirm that the data supporting the findings of this study are available within the article and its Supplementary material. Raw data that support findings of this study are available from the corresponding author, upon reasonable request.

Competing interests Not applicable

Funding This research is funded by Vietnam National University Ho Chi Minh City (VNU-HCM) under grant number C2021-20-15.

Authors' contributions Trong-Tai Nguyen conceived of the presented idea, developed the theory and performed the computations, prepared facilities for experimental, verified the analytical methods and results. Quang-Tho Le, Quang-Phuoc Pham, Tran-Long Le conducted experimental results. All authors discussed the results and contributed to the final manuscript.

ACKNOWLEDGEMENTS

We acknowledge the support of time and facilities from Ho Chi Minh City University of Technology (HCMUT), VNU-HCM for this study.

AUTHORS

Trong-Tai Nguyen* – Faculty of Electrical and Electronics Engineering, Ho Chi Minh City University of Technology (HCMUT), Vietnam National University Ho Chi Minh City, Ho Chi Minh City, Vietnam, email: nttai@hcmut.edu.vn.

Quang-Tho Le – Faculty of Electrical and Electronics Engineering, Ho Chi Minh City University of Technology (HCMUT), Vietnam National University Ho Chi Minh City, Ho Chi Minh City, Vietnam, email: tholequang480@gmail.com.

Quang-Phuoc Pham – Faculty of Electrical and Electronics Engineering, Ho Chi Minh City University of Technology (HCMUT), Vietnam National University Ho Chi Minh City, Ho Chi Minh City, Vietnam, email: soattag@gmail.com.

Tran-Long Le – Faculty of Electrical and Electronics Engineering, Ho Chi Minh City University of Technology (HCMUT), Vietnam National University Ho Chi Minh City, Ho Chi Minh City, Vietnam, email: tranlong792001@gmail.com

*Corresponding author

References

[1] R. Galati, G. Mantriota, and G. Reina, "Adaptive Heading Correction for an Industrial Heavy-Duty Omnidirectional Robot," *Sci Rep,* vol. 12, no. 1, 2022, p. 19608.

[2] D. Eck et al., "A Evaluation Test Bed for Outdoor Localization Algorithms Using a High-Precision Positioning System," *IFAC-PapersOnLine,* vol. 48, no. 10, 2015, pp. 34-40.

[3] I. Doroftei and B.-d.D. Mangeron, "Practical Applications for Mobile Robots Based on Mecanum Wheels - A Systematic Survey," 2011.

[4] J.P. Trevelyan, S.-C. Kang, and W. R. Hamel, "Robotics in Hazardous Applications," *Springer Handbook of Robotics*, B. Siciliano and O. Khatib, eds., Springer Berlin Heidelberg, 2008, pp. 1101–1126.

[5] N. N, B.U. Balappa, and S. Ravichandran, "Design and Development of Vision Based Mobile Robot for Warehouse Application," *2023 IEEE North Karnataka Subsection Flagship International Conference* (NKCon), 2023, pp. 1–6.

[6] O. Buckmann, M. Krömker, and U. Berger, "An Application Platform for the Development and Experimental Validation of Mobile Robots for Health Care Purposes," *Journal of Intelligent and Robotic Systems,* vol. 22, no. 3, 1998, pp. 331–350.

[7] F. Adăscăliţei and I.J.T.R.R.P.M. Doroftei, "Practical Applications for Mobile Robots based on Mecanum Wheels-A Systematic Survey," vol. 40, 2011, pp. 21–29.

[8] O. Setiadilaga, A. Cahyadi, and A. Ataka, "Mecanum-Wheeled Robot Control based on Deep Reinforcement Learning," *2023 15th International Conference on Information Technology and Electrical Engineering* (ICITEE), 2023, pp. 25–30.

[9] J. Leng et al., "Design, Modeling, and Control of a New Multi-Motion Mobile Robot based on Spoked Mecanum Wheels," *Biomimetics,* vol. 8, no. 2, 2023, p. 183.

[10] C.-H. Kuo, "Trajectory and Heading Tracking of a Mecanum Wheeled Robot using Fuzzy Logic Control," *2016 International Conference on Instrumentation, Control and Automation* (ICA), 2016, pp. 54–59.

[11] G. Bayar and S. Ozturk, "Investigation of the Effects of Contact Forces Acting on Rollers of a Mecanum Wheeled Robot," *Mechatronics,* vol. 72, 2020, p. 102467.

[12] T.D. Nguyen, D.P. Dinh, and T.H. Tran, "Kinematic Modeling and Stable Control Law Designing for Four Mecanum Wheeled Mobile Robot Platform Based on Lyapunov Stability Criterion," *Journal of Technical Education Science,* vol. 18, no. 5, 2023, pp. 57–65.

[13] S. Mellah et al., "Trajectory Reconfiguration for Time Delay Reduction in the Case of Unexpected Obstacles: Application to 4-Mecanum Wheeled Mobile Robots (4-MWMR) for Industrial Purposes," *IFAC-PapersOnLine,* vol. 53, no. 2, 2020, pp. 15653–15658.

[14] P. Manzl, M. Sereinig, and J. Gerstmayr, "A Mecanum Wheel Model based on Orthotropic Friction with Experimental Validation," *Mechanism and Machine Theory,* vol. 193, 2024, p. 105548.

[15] N.H. Thai, T.T.K. Ly, and L.Q. Duzung, "Trajectory Tracking Control for Mecanum Wheel Mobile Robot by Time-Varying Parameter PID Controller," *Bulletin of Electrical Engineerign and Informatics*, vol. 11, no. 4, 2022, pp. 1902–1910, 2022.

[16] G. Cao et al., "Fuzzy Adaptive PID Control Method for Multi-Mecanum-Wheeled Mobile Robot," *Journal of Mechanical Science and Technology,* vol. 36, no. 4, 2022, pp. 2019–2029.

[17] B. Wen et al., "Research on Trajectory Tracking Control Method of Omnidirectional Moving Platform based on Backstepping," *Journal of Physics: Conference Series*, vol. 1828, no. 1, 2021, p. 012141.

[18] A. Bessas, A. Benalia, and F. Boudjema, "Integral Sliding Mode Control for Trajectory Tracking of Wheeled Mobile Robot in Presence of Uncertainties," *J Control Sci Eng,* 2016.

[19] M. Szeremeta and M.J.A.S. Szuster, "Neural Tracking Control of a Four-Wheeled Mobile Robot with Mecanum Wheels," vol. 12, no. 11, 2022, p. 5322.

[20] T.T.K. Ly et al., "A Neural Network Controller Design for the Mecanum Wheel Mobile Robot," *Engineering, Technology & Applied Science Research,* vol. 13, no. 2, 2023, pp. 10541–10547.

[21] S.A. Ahmed and M.G. Petrov, "Trajectory Control of Mobile Robots using Type-2 Fuzzy-Neural PID Controller," *IFAC-PapersOnLine,* vol. 48, no. 24, 2015, pp. 138-143.

[22] Q. Jia et al., "Motion Control of Omnidirectional Mobile Robot Based on Fuzzy PID," *2019 Chinese Control And Decision Conference* (CCDC), 2019, pp. 5149-5154.

[23] I. Sajad Ahmad Wani et al., "Motion Control of Autonomous Mobility System Using Fuzzy-PID Controller," *Tuijin Jishu/Journal of Propulsion Technology,* vol. 45, no. 2, 2024, pp. 5402–5416.

[24] H. Chen, "Fuzzy PID-based Temperature Control Method for Power Transformer Coils," *International Journal of Energy Technology and Policy,* vol. 19, no. 1-2, 2024, pp. 86–104.

[25] G. Ji et al., "Research on Variable Universe Fuzzy PID Control for Semi-Active Suspension with CDC Dampers Based on Dynamic Adjustment Functions," *Scientific Reports,* vol. 14, no. 1, 2024, p. 3442.

[26] B. Zhang et al., "Fuzzy PID Control of Permanent Magnet Synchronous Motor Electric Steering Engine by Improved Beetle Antennae Search Algorithm," *Scientific Reports,* vol. 14, no. 1, 2024, p. 2898.

[27] Y.-H. Chen and Y.-Y. Chen, "Nonlinear Adaptive Fuzzy Control Design for Wheeled Mobile Robots with using the Skew Symmetrical Property," *Symmetry*, vol. 15, no. 1; doi: 10.3390/sym15010221

[28] M.B. Alatise and G.P.J.S. Hancke, "Pose Estimation of a Mobile Robot based on Fusion of IMU Data and Vision Data using an Extended Kalman Filter," vol. 17, no. 10, 2017, p. 2164.

[29] A. Noordin, M. Basri, and Z.J.T. Mohamed, "Sensor Fusion Algorithm by Complementary Filter for Attitude Estimation of Quadrotor with Low-Cost IMU," vol. 16, no. 2, 2018, pp. 868–875.

[30] F. Guangrui and W. Geng, "Vision-based Autonomous Docking and Re-charging System for Mobile Robot in Warehouse Environment," *2017 2nd International Conference on Robotics and Automation Engineering* (ICRAE), 2017, pp. 79-83.

[31] J. Huang et al., "Indoor Positioning Systems of Mobile Robots: A Review," *Robotics*, vol. 12, no. 2; doi: 10.3390/robotics12020047

[32] H. Di and Z. Chu, "Design of Indoor Mobile Robot based on ROS and lidar," *Proceedings of the 2022 2nd International Conference on Robotics and Control Engineering, Nanjing, China, 2022*; doi:10.1145/3529261.3529272

[33] R. Raj and A. Kos, "A Comprehensive Study of Mobile Robot: History, Developments, Applications, and Future Research Perspectives," *Applied Sciences*, vol. 12, no. 14; doi: 10.3390/app12146951

[34] P. Tripicchio, S. D'Avella, and M. Unetti, "Efficient Localization in Warehouse Logistics: A Comparison of LMS Approaches for 3D Multilateration of Passive UHF RFID tags," *The International Journal of Advanced Manufacturing Technology,* vol. 120, no. 7, 2022, pp. 4977–4988.

[35] Y. Liu et al., "A Review of Sensing Technologies for Indoor Autonomous Mobile Robots,", *Sensors (Basel),* vol. 24, no. 4, 2024.

[36] B. Alsadik, "Chapter 10 - Kalman Filter," *Adjustment Models in 3D Geomatics and Computational Geophysics*, B. Alsadik, ed., Elsevier, vol. 4, 2019, pp. 299–326.

[37] M.K. Hoang et al., "A Hidden Markov Model for Indoor User Tracking based on WiFi Fingerprinting and Step Detection," *21st European Signal Processing Conference* (EUSIPCO 2013), 2013, pp. 1–5.

[38] X. Ren et al., "An Improved Hidden Markov Model for Indoor Positioning," *Communications and Networking*, Springer Natrure, 2023, pp. 403–420.

[39] A.I. Sudianto, M.A. Muslim, and M. Rusli, "Sensor Fusion using Model Predictive Control for Differential Dual Wheeled Robot," *Kinetik: Game Technology, Information System, Computer Network, Computing, Electronics, and Control,* vol. 8, no. 1, 2023, pp. 461–472.

[40] V.L. Popov et al., "Detection and Following of Moving Target by an Indoor Mobile Robot using Multi-sensor Information," *IFAC-PapersOnLine,* vol. 54, no. 13, 2021, pp. 357–362.

[41] A.T. Erdem and A.Ö.J.I.T.O.I.P. Ercan, "Fusing Inertial Sensor Data in an Extended Kalman Filter for 3D Camera Tracking," vol. 24, no. 2, 2014, pp. 538–548.

[42] A. Cavallo et al., "Experimental Comparison of Sensor Fusion Algorithms for Attitude Estimation," vol. 47, no. 3, 2014, pp. 7585–7591.

[43] S.O. Madgwick, A.J. Harrison, and R. Vaidyanathan, "Estimation of IMU and MARG Orientation using a Gradient Descent Algorithm," *2011 IEEE international conference on rehabilitation robotics*, 2011, pp. 1–7.

[44] D. Parikh, S. Vohra, and M. Kaveshgar, "Comparison of Attitude Estimation Algorithms with IMU Under External Acceleration," *2021 IEEE International Symposium on Smart Electronic Systems* (iSES), 2021, pp. 123–126.

[45] R. Mahony, T. Hamel, and J.-M.J.I.T.o.a.c. Pflimlin, "Nonlinear Complementary Filters on the Special Orthogonal Group," vol. 53, no. 5, 2008, pp. 1203–1218.

[46] J. Zheng et al., "Visual Localization of Inspection Robot using Extended Kalman Filter and Aruco

Markers," *2018 IEEE International Conference on Robotics and Biomimetics* (ROBIO), 2018, pp. 742–747.

[47] S. Roos-Hoefgeest, I.A. Garcia, and R.C. Gonzalez, "Mobile Robot Localization in Industrial Environments using a Ring of Cameras and ArUco Markers," *IECON 2021 – 47th Annual Conference of the IEEE Industrial Electronics Society*, 2021, pp. 1–6.

[48] Z. Yuan et al., "Trajectory Tracking Control of a Four Mecanum Wheeled Mobile Platform: An Extended State Observer-based Sliding Mode Approach," *IET Control Theory & Applications,* vol. 14, no. 3, 2020, pp. 415–426.